AFOSR-TR-97-0589

REPORT DOCUMENTATION PAGE

Form Approved
OMB No. 0704-0188

1. AGENCY USE ONLY (Leave blank)	2. REPORT DATE	3. REPORT TYPE AND DATES COVERED
	14 Oct 97	Final 15 Aug 94 - 14 Aug 97

4. TITLE AND SUBTITLE
INORGANIC-ORGANIC MOLECULAR BONDING IN POROUS MATRICES

5. FUNDING NUMBERS
F49620-94-1-0295
3484/XS
61103D

6. AUTHOR(S)
L. L. Hench

7. PERFORMING ORGANIZATION NAME(S) AND ADDRESS(ES)
University of Florida
219 Grinter Hall
Gainesville, FL 32611

8. PERFORMING ORGANIZATION REPORT NUMBER

9. SPONSORING / MONITORING AGENCY NAME(S) AND ADDRESS(ES)
AFOSR/~~NC~~ NL
110 Duncan Avenue Suite B115
Bolling AFB DC 20332-001
Maj Hugh C. DeLong

10. SPONSORING / MONITORING AGENCY REPORT NUMBER
F49620-94-1-0295

11. SUPPLEMENTARY NOTES

12a. DISTRIBUTION / AVAILABILITY STATEMENT
APPROVED FOR PUBLIC RELEASE; DISTRIBUTION IS UNLIMITED.

12b. DISTRIBUTION CODE

13. ABSTRACT *(Maximum 200 words)*

The use of porous gel-silica matrices as host materials for optical sensors, catalyst supports, and organic-inorganic composite materials has received increased attention over the past several years. Porous, optically transparent hosts have several advantages over traditional materials for these applications. Large surface areas inherent in sol-gel derived silica increase the interaction area for surface mediated reactions while large pore volumes enhance the introduction of organic or inorganic modifiers or analyzates into the glass substrate. The ability to produce larger pores in these materials increases the permeability and environmental stability of the substrates and enhances the introduction of second phases as modifiers. Greater permeability also increases the responsiveness of sensors and efficiencies of catalyst materials. Previous efforts have produced and characterized gel-silica matrices with average pore diameters from 2.4nm to 20nm. With recent advances, gel-silica matrices have now been fabricated with average pore diameters as large as 80nm using conventional drying techniques. The introduction of CO_2 supercritical drying of matrices has enhanced the ability to specifically tailor the surface area and pore volume. The feasibility of doping with metal salts and colloids has been demonstrated as well as the ability to produce dense silica optical components.

14. SUBJECT TERMS	15. NUMBER OF PAGES
Glass, surfaces, optics, aging, sol-gel, gels, porous glass, aerogel, processing, composites,	58
	16. PRICE CODE

17. SECURITY CLASSIFICATION OF REPORT	18. SECURITY CLASSIFICATION OF THIS PAGE	19. SECURITY CLASSIFICATION OF ABSTRACT	20. LIMITATION OF ABSTRACT
UNCLASSIFIED	UNCLASSIFIED	UNCLASSIFIED	

ASSERT94

INORGANIC-ORGANIC MOLECULAR BONDING IN POROUS MATRICES

FINAL REPORT

to

AIR FORCE OFFICE OF SCIENTIFIC RESEARCH
Bolling Air Force Base, DC 20332

Grant No. F49620-94-1-0295

Period Covered

SEPTEMBER 15, 1996 - September 14, 1997

Submitted by

L.L. Hench, Principal Investigator

Department of Materials Science and Engineering
University of Florida
P.O. Box 116400
Gainesville, Florida 32611-6400

TABLE OF CONTENTS

CHAPTER 1

LOW DENSITY XEROGELS IN THE SPECTRUM OF POROUS GLASSES

1.1 Porous Silica Glasses.

Porous silicate glasses are produced by two primary methods. The first method is to produce a phase separated glass with two continuous phases and then leach out one of the phases with an appropriate corrosive fluid. This is how Corning Inc produces Vycor® brand porous high silica glass. The second method and the primary subject of this report is sol gel type glasses which are produced by the controlled gelation of colloidal silica particles or the hydrolysis and condensation of various silicon alkoxides. The sol gel method of producing porous glasses is by far the more flexible of the two for producing a range of properties in the porous glass product. Surface areas, pore volumes, bulk densities and pore sizes can all be engineered through the manipulation of the reaction conditions and post-gelation thermal treatments.

Porous glasses have several unique characteristics which promise to make them a very significant part of our technological bag of tricks. They can be crafted with large surface areas, pore diameters from 1.5 nm to several microns, pore volumes of up to 95%, and densities from .005g/cm^3 up to the full density of fused silica (2.2g/cm^3). They can be synthesized with 99.99+ % purity through the use of silicon alkoxide precursors and doped with virtually any material that can be introduced as a liquid or a gas. They can be made transparent, translucent or opaque by manipulating the pore size and or

incorporating second phases. High purity silica is stable in all but the most severe aqueous environments and are impervious to most organic solvents. Porous silica is also thermally stable and can maintain their porosity up to 1000°C. [1]

1.2 Vycor® and Phase Separated Glasses

Vycor® is the brand name for the phase separated glass products produced by Corning Incorporated. The production of Vycor® is based on the work of Hood and Nordberg .[2,3] Vycor® type glasses can be made by taking advantage of the phase separation in the silica - borate - soda system. A multicomponent glass is produced consisting of 65% silica, 27% B_2O_5, and 8% Na_2O which is cast in the desired shape. Upon cooling the glass phase separates into two phases, a silica rich phase and a boron/sodium rich phase. Upon further heat treatment, the phases consolidate into two interconnected phases, the size and morphology of which increase with time and temperature. After cooling, the boron/sodium rich phase is leached out of the glass using a hot dilute acid mixture which reacts with the borate and sodium constituents to form soluble species. This is a time consuming operation especially as the thickness of the sample increases. The silica rich phase remains unaffected by the acid solution. The resulting product is a porous glass consisting of approximately 96% silica, 3% B_2O_5, and 1% Na_2O and trace impurities. Once the boron and sodium rich phase is etched out, the product is washed to remove the acid solution and dried. The remaining glass has an interconnected porosity with chemical and physical characteristics similar to pure silica. Table 1.1 lists the composition of a typical phase separated porous glass and Table 1.2 depicts some of its properties.[4] Vycor® is often cast in various shapes, treated as described above to form a porous preform, and consolidated at high temperatures (1200°C) to form a dense, low expansion glass with properties nearly identical to fused silica.

Table 1.1 Composition of Typical Phase Separated Vycor® Glass.[4]

Composition of Vycor®	
Oxide	Wt/% Composition
SiO_2	96.6%
B_2O_3	2.95%
Na_2O	.4%
$R_2O_3 + RO_2$	<.1%

Table 1.2. Typical Properties of Corning Brand (7930) Vycor® Glass.[4]

Properties of Vycor®	
Appearance	Opalescent
Refractive Index	1.33
Bulk Density (g/cm^3)	1.5
Pore Volume (%)	28
Avg. Pore Diameter (Å)	50
Spec Surf Area (m^2/g)	200
Mod of Rupture (MPa)	42
Young's Modulus at 22°C GPa	17.6

1.3 Alkoxide Derived Silica Gels.

Sol Gel processing of ceramic materials (silica) traces its history back over 100 years to the mid 19th century with the work of Ebelmen and Graham and their study of aqueous colloidal suspensions of silica.[5] Over the ensuing 15 decades a great deal of progress has been made in characterizing silica suspensions and in the basic understanding of the physical and chemical processes that occur between solution and glass. R.K. Iler has written a comprehensive treatise on the properties of silica in The Chemistry of Silica.[6] The properties of silica in aqueous solutions are of prime importance for understanding the sol gel process.

In the last two decades, great excitement has been generated through the increasing use of silicon alkoxides, primarily tetraethoxysilane (TEOS) and tetramethoxy silane, (TMOS) as precursors in producing silica gels and other colloidal products. It is due in no small part to this flurry of investigation into silica gels that the production and study of a wide variety of metal alkoxides and mixed component alkoxides has dramatically increased over the past decade. Over the past twenty years literally thousands of journal articles, proceedings, books and other communications have been written regarding the study of sol-gel derived glasses.

More recently Scherer and Brinker have attempted to consolidate the principles of sol gel physics and chemistry in their book Sol gel Science. [7] An even more recent resource on the latest developments in the science is the book The Colloidal Chemistry of Silica, edited by H.E. Bergna for the American Chemical Society.[8]

The sol gel process is a product of several unique aspects of aqueous silica chemistry including the low solubility of silica over a wide pH range, the ease in which a solution can be supersaturated with silica, the large surface charge formed on the surface of colloidal silica in aqueous solutions, and the propensity for silanol groups to undergo the condensation reaction to form highly stable siloxane bonds. In alkoxide derived silica

gels, a number of variables can be manipulated to customize the properties of the resulting glass. The primary variables include: the ratio of alkoxide to water (R-ratio), pH, the solvent system, conditions of gelation, the addition of catalysts or other additives, aging times and temperatures, method of drying, and high temperature (stabilization) treatments. Consequently, porous glasses derived from the sol gel process can be synthesized with a much wider range of surface areas, pore volumes and pore diameters than Vycor® type glasses which are limited by the stoichiometry of the separated phases. The primary drawback of the sol gel process is the difficulty in drying monolithic, net shape pieces. Porous glasses of all types are prone to cracking due to the large capillary stresses encountered during the drying process. Residual water can also be a problem when dense silica components are produced by high temperature consolidation. Much of the literature is devoted to understanding the principles involved in the sol gel process in order to address these problems.

1.4 The Surface Area of Porous Glasses.

Because of the small scale of their porosity, porous glasses have large specific surface areas. A typical Vycor® type glass as noted in Table 1.2 will have a surface area of around 200 square meters per gram of material. Sol gel derived glasses can have surface areas in excess of 1000 m^2/g. Four grams of this material contains more surface area than a football field. Indeed some aerogels have been measured with surface areas of over 1700 m^2/g.[9] Surface areas of this magnitude present a situation in which the bulk physical properties of the material begin to become dominated by its surface properties. Many surface phenomena that hitherto went unnoticed can now be studied, characterized and applied toward new technologies. Such large surface areas , for example, are important in many applications such as catalyst substrates and surface mediated chemical processes. The optical properties of surface states is another area which is receiving increased

attention as the ability to generate large surface areas in transparent media becomes more prevalent.[10]

1.5 Pore Volume.

The available pore volume of phase separated glasses is limited by the stoichiometric proportions of the constituents and the composition of the boron rich phase which is etched out of the phase separated glass. Thus the pore volume is limited to the general vicinity of 25%. Larger pore volumes can be achieved through etching with hydrofluoric acid solutions however this abnormally increases the pore size and increases the length and complexity of the synthesis.[11] Sol gel derived glasses provide much more flexibility in terms of selecting and producing the pore volume desired for a specific application. In this study, pore volumes ranging from 25% to 80% are routinely produced in xerogels while porosity as high as 95% have been produced through aerogel technology. Combining the two types of processing can yield pore volumes tailored to any intermediate point.

1.6 Pore Size.

Porous glasses are generally characterized by mercury intrusion or nitrogen adsorption which provide relatively accurate surface area and pore volume determinations. Each technique has its own advantages and limitations. Mercury intrusion requires very high pressures to measure small pores and gives little information on the micropore content of a material. By contrast, nitrogen adsorption is limited to pores less than about .1 micron in diameter.[12,13,14] Pore sizes are generally computed in terms of the hydraulic pore

diameter which assumes uniform cylindrical pores a morphology which seldom occurs in either phase separated glasses or sol gel derived glasses. Even so, the hydraulic pore size is a convenient way of comparing the porosities of different materials. The average pore size is computed using the following equation:

$$r = \frac{2 \cdot V_p}{S.A.} \tag{1}$$

where r is the pore radius, V_p is the specific pore volume and S.A. is the specific surface area of the material. Care must be taken not to take this model too literally as the pores are not usually uniform nor cylindrical in shape. Vycor® type porous glasses generally produce pore sizes in the range of 4 nanometers but can be etched to sizes on the order of 20 nanometers. Xerogels can be produced with a wide range of pore sizes from less than 2 nanometers to nearly 100 nanometers. Larger pore sizes are normally produced through aging or etching treatments as with the phase separated glasses.[15] Although pore size is a convenient characteristic of a porous glass it should always be considered in context with the pore volume and surface areas from which it is derived.

1.7 Consolidation

The objectives of this study grew out of the desire to create and characterize porous silica gel matrices or substrates suitable for use in the production of optical sensors. The desired characteristics included a large surface area, large pore openings, sufficient transparency to visible light, and stability under a wide variety of chemical environments. As work progressed toward these goals it became apparent that these substrates also showed promise as preforms for densification into fused silica pieces and

homogeneous doped silica glasses. The production of net shape dense fused silica fixtures and optical components has been the "Holy Grail" of porous glass producers ever since it was discovered that these glasses could be consolidated into dense glass at temperatures much lower than that required for melt derived glasses.[7] Due to the extremely high working temperatures (2000°C) and high viscosity of pure silica, it is difficult and expensive to produce via traditional melt technology. Precision shapes are difficult to form, homogeneity suffers and purity is insufficient due to contamination from refractories and retained water. Thus the consolidation of porous glasses at lower temperatures is an attractive alternative.

Vycor® type glass has been used for many years for this purpose but still suffers from several drawbacks.. It still must be cast from a molten state and thus requires high temperatures and energy costs. The borate rich phase must be chemically etched out of the glass, a time consuming and not always successful process. After the etching process is complete drying the glass is difficult, especially for thick pieces and Vycor® still contains up to 4% sodium and borate in the final dense product.

Silica gels have always and continue to suffer from drawbacks as well, primarily, the inability to dry large net shaped pieces intact. Drying monolithic gels intact is a time consuming and fickle operation. The larger the piece, the more difficult and time consuming it is to dry without cracking or warping. Although thermally densified silica gel pieces are much purer than Vycor®, they to tend to retain water due to their large hydrated surface which can result in bloating. Even when successfully densified, Sol gel derived fused silica still can contain a few parts per million water. Though this doesn't

seem like much it is still insufficient purity for many high tech applications such as in the fiber optic industry.[16]

1.8 Research Objectives

Due to the remarkable properties of the xerogels described herein, the objectives of this research incorporated the following:

1. Develop and characterize a monolithic porous silica gel substrate suitable for use in optical sensors. Such a substrate should have a large surface area, large pores with good permeability, sufficient mechanical strength to survive rehydration forces encountered during doping and during use, environmental stability, and adequate optical transparency in the visible spectrum.

2. Improve on the ability to create large net shape dried monolithic silica pieces suitable for dehydration treatments and densification into high purity dense fused silica pieces. Study the aging characteristics of porous sol gel matrices to maximize strength and minimize retained water. Homogeneity should be sufficient for use in optical applications.

1.9 Summary

Chapter 2 reports on the progress made toward producing xerogel matrices with larger pores and pore volumes. Larger pores are desirable from the standpoint of lower capillary forces during drying and lower surface areas (hence less retained water). Although pore diameters of up to 80 nanometers have been fabricated the optical properties in the visible tend to deteriorate due to Rayleigh scattering. Consequently emphasis has been concentrated on 40 nanometer substrates. The processing parameters and properties have been well characterized and are predictable. Although dry 40 nanometer substrates exhibit significant optical scattering, transparency increases to acceptable levels when they are filled with an aqueous or organic solvent as would be the case for most sensor applications.

Chapter 3 explores some fundamental processing issues particularly the changes in pore morphology through the aging and drying stages of gel processing. Supercritical CO_2 drying is used to produce aerogels at different stages in the aging process allowing a precise analysis of the pore structures in this processing regime.

Despite the massive amount of research that has been conducted over the last few decades, sol gel science still has many questions in need of investigation and fruitful areas for advancement. The use of sol gel technology for the production of high purity silica products is still in need of development. Potential applications in the field of optical sensing and catalyst supports also show promise and with the advent of aerogel technology sol gel produced glass has good potential as a highly efficient transparent insulating material. Regardless of the application, the fundamental aging ,drying and consolidation processes must be understood in order to tailor the porous glass to its intended use.

CHAPTER 2
SOL GEL PROCESSING OF LARGE MESOPORE SILICA MONOLITHS

2.1 Introduction

There are a variety of methods for making large pore silica gels starting from a variety of precursors.[7] The term "large pore" is relative but is used here to refer to any gel with a pore radius greater than 10nm. In generally accepted terminology these large pore gels are still considered mesoporous. The gels in this study have pores ranging from 10 to 40 nanometers in radius. What distinguishes these gels from those produced elsewhere is that they can be produced in a single step as monoliths with very narrow pore size distributions. There is no need for base aging or acid etching thus reducing processing time and preserving better homogeneity, pore size distribution and optical properties. Optical transparency in the visible depends on the pore size due to Rayleigh scattering. Air filled monoliths retain a certain degree of optical transparency well into the visible and transmission increases accordingly when they are filled with a solvent or doped with higher refractive index materials. The size of the pores and large pore volume allows doping with a wide variety of materials to form chemical sensors, solution hosts and nanocomposite materials. Depending on the nature of the dopant, the resulting composite can be used in optical applications in the visible and near IR regions. Unlike smaller pore sizes these large pore gels retain enough strength (relative to capillary forces) to be rehydrated after drying without the failure of the monolith. The ability to rehydrate the gels without high temperature stabilization treatments allows organic and other temperature sensitive dopants to be introduced during gelation and retained intact in the dried gels. If pre-doping is not required and greater strength is desired the gels can be stabilized at a variety of temperatures up to 1150°C where they generally achieve full

density. As stabilization temperature increases pore size remains fairly constant up through 1000°C while pore volume decreases only slightly. Structural hardness increases with increasing stabilization temperature.

2.2 Gel Processing.

The flow chart in Figure 2.1 shows the basic steps in producing silica gel monoliths. The first step is to select the silica source. Gels can be made from sodium silicates, colloidal silicas such as Ludox, or a variety of silicon alkoxides. The most common alkoxide precursors are tetraethoxysilane (TEOS) and tetramethoxysilane (TMOS). TMOS was chosen in this system due to its rapid hydrolysis. The use of fluoride as a catalyst dramatically speeds the condensation (gelation) thus it is convenient to have rapid and complete hydrolysis in order to better control the kinetics. All of the gels discussed here are condensation limited. After gelation, the aging and drying steps of the process are the second major determinant of pore size and texture. It cannot be over emphasized that aging continues during drying as long as there is water in the gel. In fact with the higher temperatures involved in drying it may very well be the predominant aging step. This will be explored further in the next chapter. After drying the gels can be used in their dry state or further modified by doping them with the desired material. A big advantage of these large pore monoliths is that they can be doped in the dry state without cracking and redried intact to produce a dried doped gel suitable for immediate use or further stabilization treatments. Stabilization involves heating the dried gels at elevated temperatures to strengthen the gel, change the surface properties or modify the pore volume and pore sizes. As temperatures approach the softening point for silica the pore network collapses due to viscous flow resulting in fully dense silica or doped silica components. For these large pore gels, dehydroxylation treatments are generally unnecessary.

2.2.1 Formulation and Mixing

Large pore silica gels can be made by HF catalysis of tetramethoxysilane (TMOS) and water in a nitric acid/methanol solution of pH 2 - 2.5. The molar ratio (R value) of water to TMOS is 16:1. Methanol is added in equal volume proportion to water. The combination of low pH, fluoride catalysis, rapid gelation and the aging/drying processes are responsible for the large pore size. The initial pore texture is controlled primarily by the conditions of gelation principally the concentration of fluoride, the pH and the R ratio. Table 2.1 presents the formulation for a variety of pore sizes. The "standard" formulation used for these studies produced an average pore radius in the vicinity of 200Å, a specific surface area of about $150m^2/g$, and a pore volume of about 1.6 cc/g when aged and dried according to the schedule in Figure 2.2. Extended periods of aging or drying, or changes in the pore liquor during aging can significantly affect the pore texture as will be discussed later. Figure 2.3 shows a photograph of a variety of 200Å monoliths. Figures 2.4 and 2.5 show the nitrogen adsorption data for a representative sample of a dried gel.

For HF gels and the larger pore sizes, gelation at room temperature can be very rapid often on the order of a few minutes. Too rapid a gelation of the sol is undesirable for several reasons including insufficient processing time, poor homogeneity, bubble formation and rapid temperature rise. In extreme cases the latter can actually result in boiloff of methanol (B.P. 65°C). Hydrolysis of TMOS is very rapid under acidic conditions. Due to its rapidity, the exothermic reaction can be considered complete when the temperature of the solution peaks and levels off. For the standard large pore system this occurs within 2 minutes. In order to increase the time available for filtering and casting the gels, the reactants are generally cooled in an ice bath to 5°C. The heat generated by hydrolysis is just enough to raise the temperature to approximately room temperature (25°C) allowing processing and gelation to occur at a stable temperature.

Table 2.1. Formulations for HF catalyzed TMOS derived monoliths.
* Indicates reactants cooled in an ice bath (≈5°C) prior to mixing.

Pore Radius Å (Nominal)	H_2O (ml)	CH_3OH (ml)	TMOS (ml)	HF (3%) (ml)	HNO_3 (1N) (ml)
30	50	0	35	1.5	10
45	50	0	35	1.5	10
100*	25	50	35	4	4
150*	25	50	35	12.5	4
200*	50	50	35	10	4
250*	50	50	35	12.5	4
400*	50	50	35	2.25 (H_2SiF_6 25%)	0

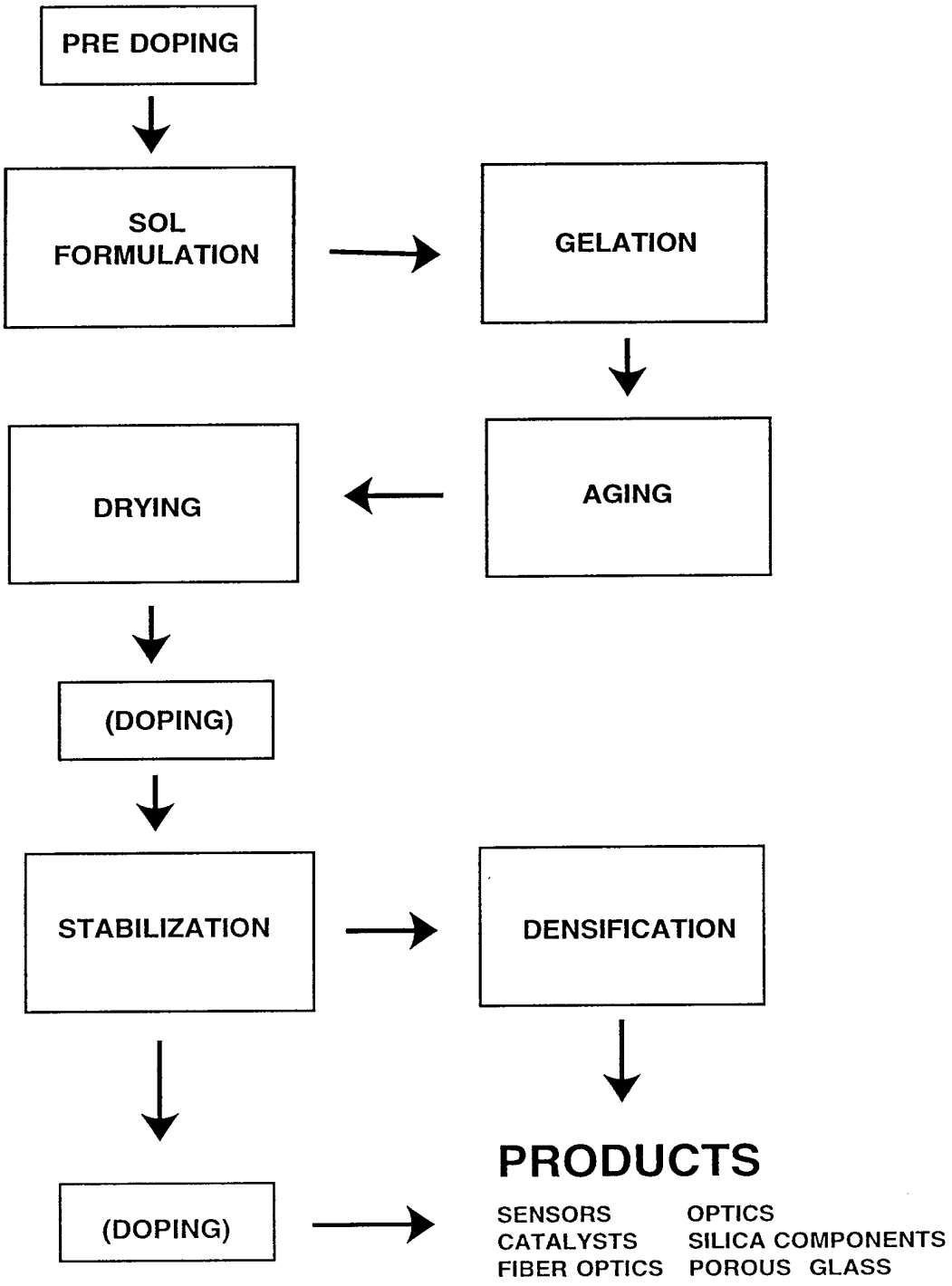

Figure 2.1. Schematic of the basic steps involved in the production of monolithic silica gel products.

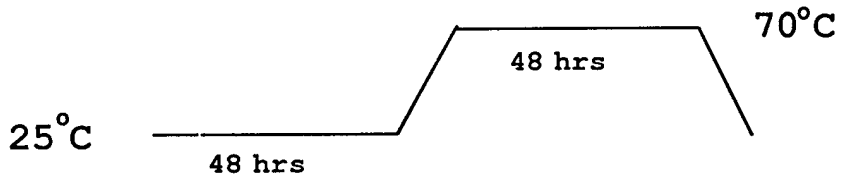

STANDARD AGING SCHEDULE

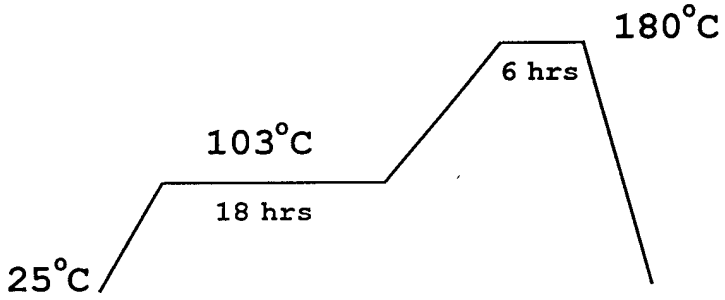

STANDARD DRYING SCHEDULE

Figure 2.2. Standard aging and drying schedules for small monoliths (2.5cm x .7cm) in the large pore system. larger monoliths require longer drying times but aging schedule is the same.

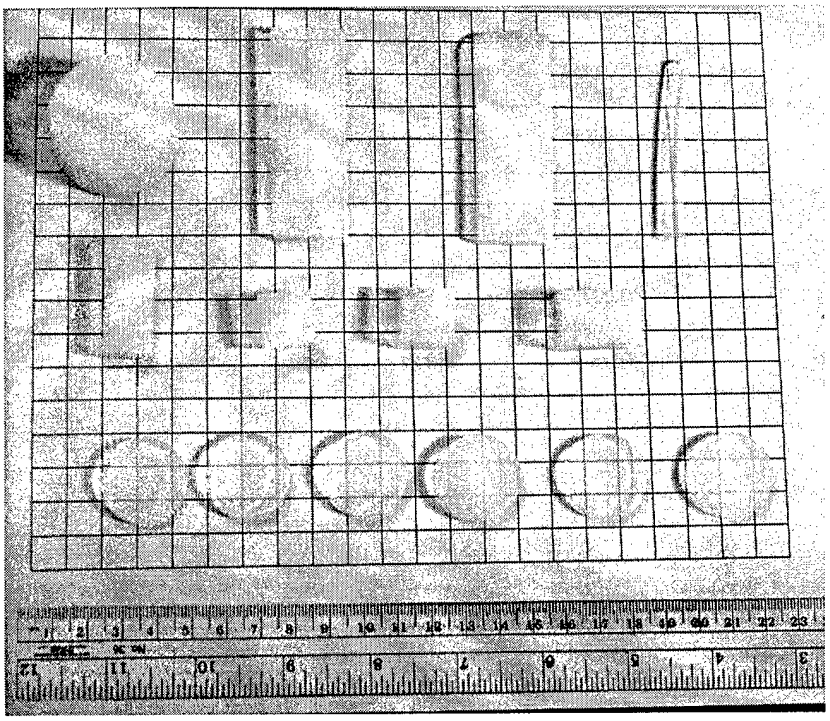

Figure 2.3. A variety of silica gel monoliths made with the "standard" formula for 200 Angstrom radius.

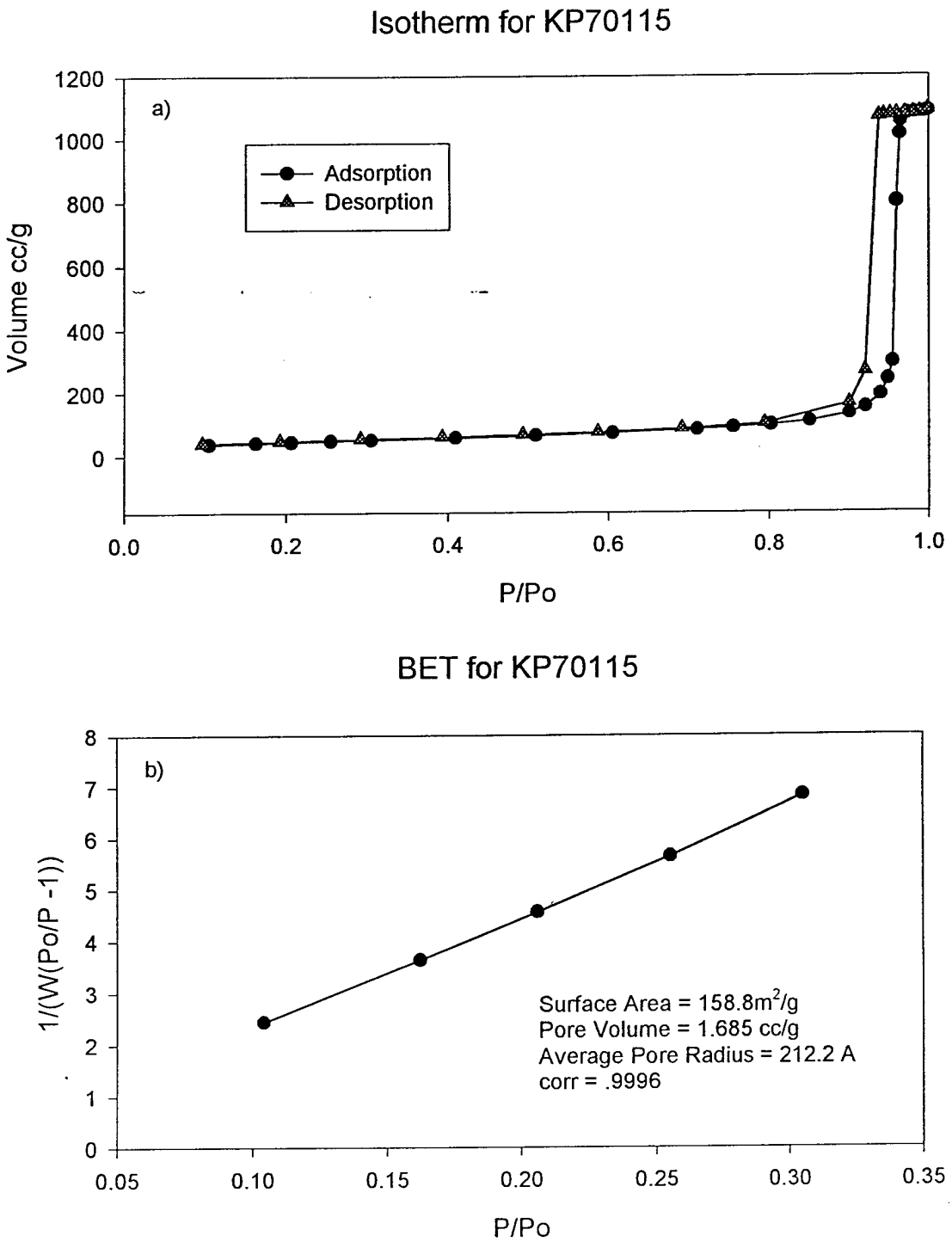

Figure 2.4. The isotherm (a) and BET plot (b) for a representative silica gel monolith made with the standard formula using the aging and drying schedules of Figure 2.2.

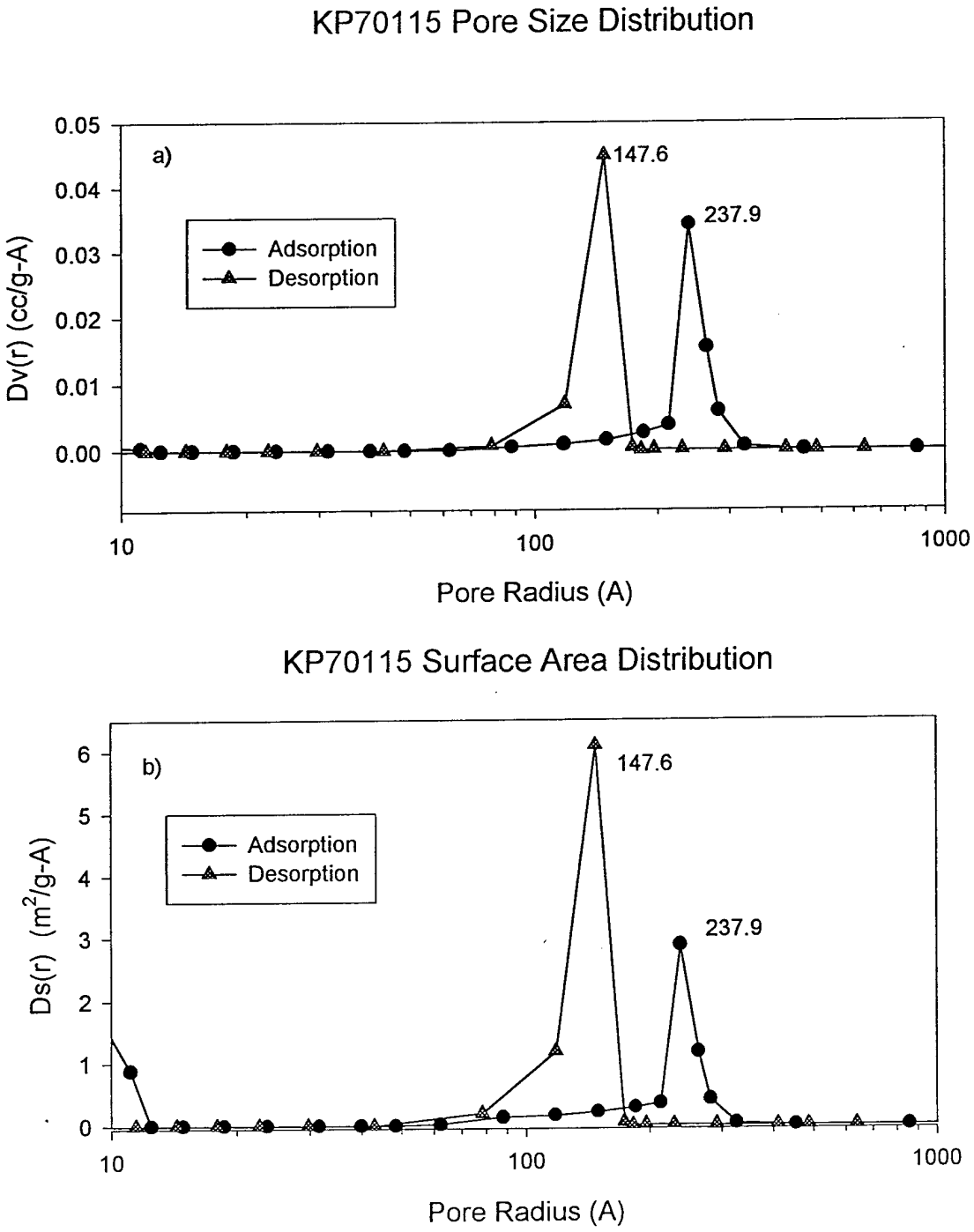

Figure 2.5. Pore size distributions (a) and surface area distributions (b) for the standard formula gel monolith in Figure 2.4. Notice the hysteresis effect between the adsorption and desorption curves. Desorption distributions are usually considered to more closely represent the equilibrium pore size.

2.2.2 Cosolvent

The addition of methanol as a cosolvent has several effects on the sol. It slows down the reaction by diluting the solution, it raises the pH of the solution, moderates the temperature rise by increasing the total thermal mass of the solution, and slows down the condensation reaction allowing more time for processing the sol.

2.2.3 Casting

The sol is allowed to stir for several minutes before being cast into polymethylpentane molds. A variety of methods can be used to effect the transfer but the most convenient found is to use a 60ml polypropylene Luer lock syringe with a 1.0 micron Teflon syringe filter. The sol is filtered to remove any dust or other particles which might serve as crack initiation sites within the gel. It is by no means proven that such particulates increase the failure rate of the monoliths and many gels have been made with good results without filtering. However prudence dictates that when possible filtering should be employed. Likewise, the presence of bubbles within the gel should be avoided whenever possible although the photo in Figure 2.6 demonstrates that bubbles are not always fatal to the gel monolith. With the short time available between mixing and gelation, filtering and casting should be done expeditiously. As the solution approaches the gelation point, the Teflon filter begins to clog and transfer becomes difficult. It is important that enough time is allowed to tightly cap the molds before gelation. If the solution gels in the open air evaporation from the surface causes a "lizard skin"- like surface on the gel. Crazing or cracking follow soon after.

2.2.4 Mold Selection

A wide variety of plastics can be used as molds for nitric acid/HF gels. Polystyrene, polypropylene, polycarbonate, polymethylpentane (PMP), and Teflon® have

all been successfully used in this study, however, polymethylpentane (PMP) is preferred. This polymer has a sufficiently smooth surface, is not attacked by TMOS, is strong enough to resist deformation when sealed during the aging process and is very hydrophobic. The latter characteristic is important in minimizing the formation of a meniscus which introduces curvature on the top surface of the gel. In sensitive gels, the meniscus often causes the top edge of the gel to break off around its circumference. Sharp, angular shapes are more difficult to dry intact for reasons which will be discussed later. Although PMP is stable up to 130°C it generally can not be used for drying due to a tendency to react with the decomposing nitric acid at the end of the drying cycle. Ideally it would be nice to dry the gels in the original mold to avoid the necessity of transferring the fragile gels to a separate drying container. This can be done in PMP if the drying temperature is lowered and the time extended however, the lower drying temperatures extends the drying time which results in a lower yield of intact gels. The presence of nitric acid at elevated temperatures attacks the polymer and release organic byproducts into the gels. Consequently, gels are normally transferred to Teflon containers for drying and are brought to a final drying temperature of 180°C. Teflon containers are sometimes used for molds but the Teflon surface is soft and does not produce a very smooth surface. Teflon is also expensive and available only in limited shapes and sizes.

2.2.5 Aging and Drying.

After casting, the gels are placed on a stable surface in an undisturbed location to age at room temperature for a minimum of 2 days. Significant syneresis (≈ 10%) occurs within an hour and continues at a lower rate throughout the aging period. The molds are then placed in an oven and aged at 70° for another 24 hours. It is important that the molds be tightly capped during this period since methanol boils at 65°C. Loss of too much solvent during the aging process results in premature drying and failure of the

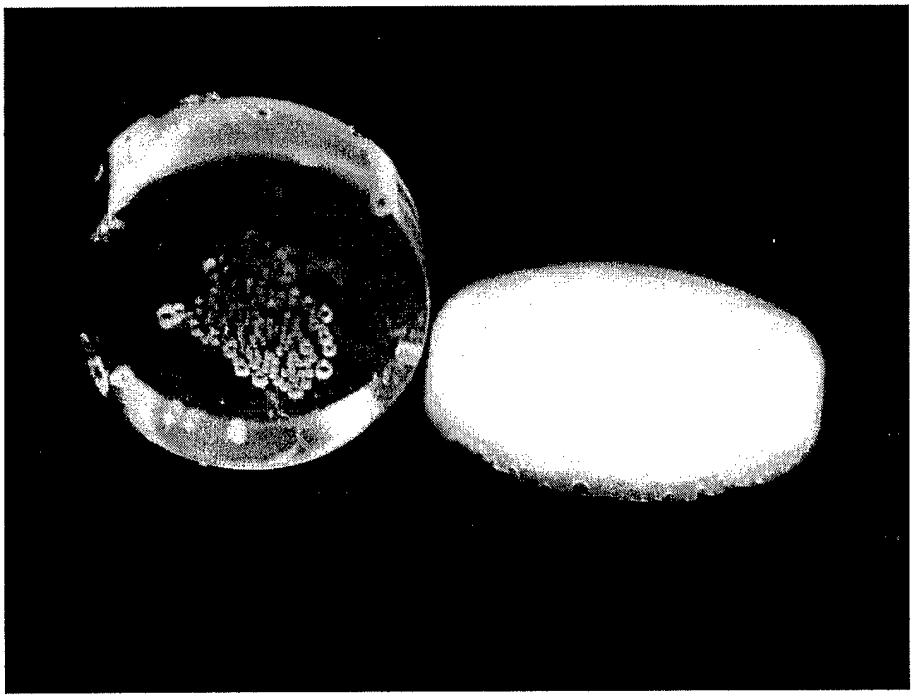

Figure 2.6. Bubbles can survive the drying process as evidenced by this photograph of two dried gel monoliths. The gel on the left has an estimated pore radius of about 20 Å while the one on the right is a standard 200Å gel.

monoliths. This aging step ensures that all unreacted silicic acid monomer is depleted. During aging and drying the gel structure undergoes Ostwald ripening especially at elevated temperatures. The pore liquor has a pH of 2 which also increases solubility of silica. Aging is a major determinant of the final gel structure (the other being the formulation).

2.2.6 Drying

The drying process used for large pore monoliths is essentially the same as with other gels except the larger pores and hence lower capillary stresses and greater permeability allows the process to be shortened to as little as 24 hours for small monoliths (25mm x 7mm). After aging, the wet gels are carefully removed from the molds and washed with deionized water. They are placed in Teflon drying containers filled with water. The function of the water is to cushion the fragile gel as it sinks to the bottom of the drying container. The water is then carefully poured out leaving only the wet gel in the bottom. The container is sealed and a small pinhole placed in a Teflon® septum. The purpose of the pinhole is to maintain a condition of near 100% humidity around the gel while it is drying. Larger monoliths are more difficult to handle and consequently are most often both cast and dried in the same Teflon container.

2.2.6.1 Drying Schedule

The drying schedule varies depending on the size of the monolith. Once the gel has survived the opaque stage, it is insensitive to the rate of further drying. After this stage is over, the gels are brought a final temperature of 180°C as this is the temperature at which most physically adsorbed water is removed. Further heating begins the stabilization process wherein proximate silanol groups condense to form water which then diffuses out of the gel.

Larger monoliths of the same basic formulation generally have lower surface areas, larger pore volumes and larger average pore sizes. Figure 2.7 is a comparison of the nitrogen adsorption analysis of three different size monoliths made with the same basic formulation. The difference in pore structure is only indirectly related to the size of the monolith. The primary determinant is the length of time the gel is subjected to the high temperature aqueous environment. Larger gels take longer to dry, hence age for a longer period, hence have larger pores and lower surface areas. Larger pores exert less capillary pressure, hence shrinkage during drying is less resulting in a larger pore volume which also contributes to a larger average pore radius. Figure 2.8 shows pieces dried in 24 hours contrasted with a large 75mm by 75mm cylinder which took 2 weeks to dry. Drying time is influenced by the size of the monolith as the water must flow/diffuse over a much longer pathlength in larger pieces.

2.2.6.2 Drying Intact Monoliths

The maximum stress on the gel occurs at the critical point i.e. the point at which the liquid begins to penetrate the pores. This is also the point at which the gels begin to turn opaque. One might initially speculate that a larger monolith should better survive the drying process since the tension applied by the liquid is applied over a longer path i.e. the center of the gel to the drying front. With the advent of large pore monoliths however, it has become apparent that the actual stress front is extends over a relatively short distance centered in the vicinity of the drying front (identified by the movement of the opaque stage). Large pore gels can be rehydrated without failure and the drying front and opaque stage observed under ambient conditions. Generally, the monolith will dry from the outside towards the center but this is not always the case as can be seen by Figure 2.9 where the opaque stage has started in the interior of the gel. Contrary to popular opinion it has also been observed that drying a gel **too slowly** can cause failure just as drying it too

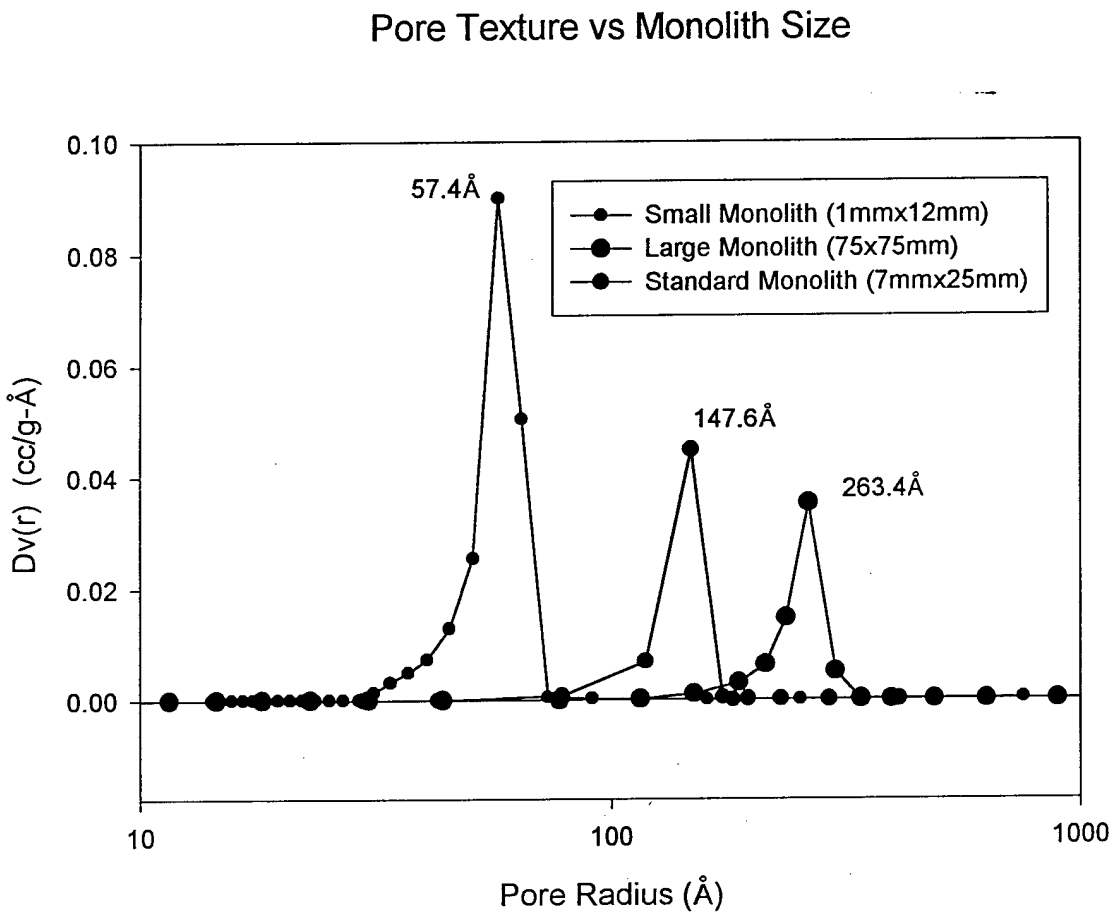

Figure 2.7. Desorption pore size distributions for three gels made with the same formulation but with different pore textures due to differences in drying schedules. The small monolith was dried in 24 hours at 60°C. the standard monolith was dried at 103°C for 24 hours and the large monolith was dried at 95°C for 2 weeks. All were treated with a 6 hour hold at a temperature of 180°C.

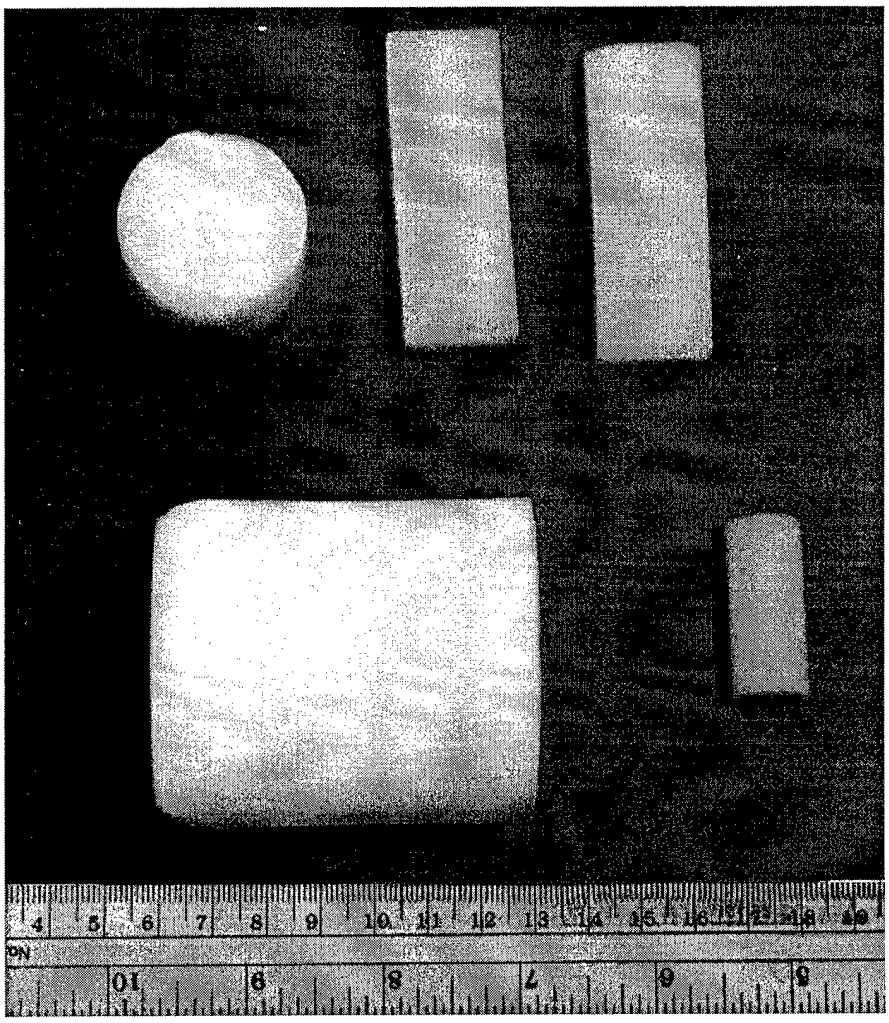

Figure 2.8. Several different size silica monoliths made with the same formulation but dried with different schedules. The small rectangular monoliths on the upper right were dried using the normal schedule while the 2 larger cylinders on the left were subject to much longer drying times. The largest cylinder took over 2 weeks to dry.

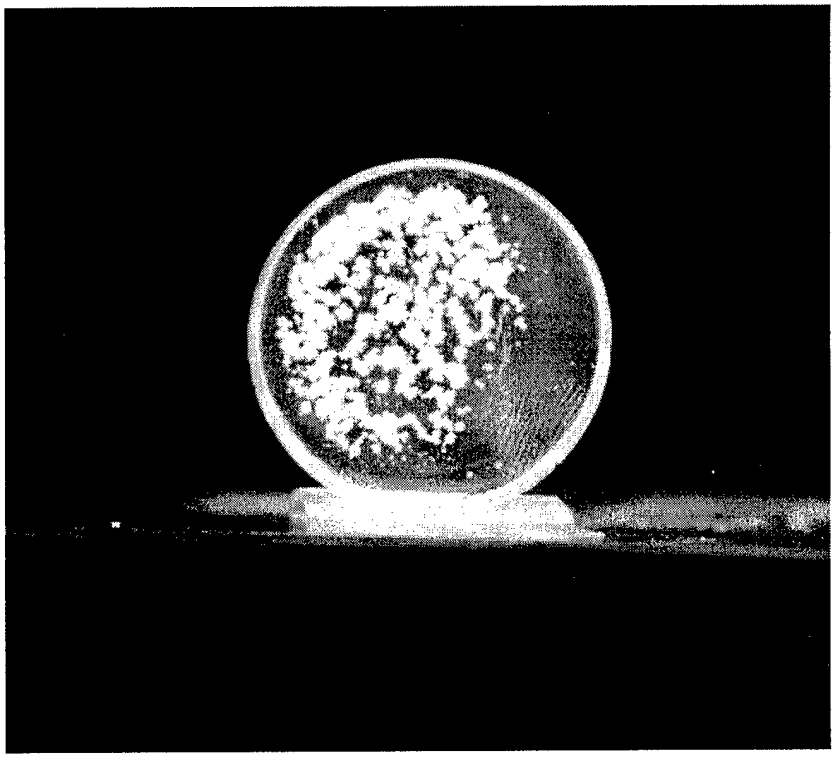

Figure 2.9. Large pore gel just beginning to enter the opaque stage during drying. Notice the cauliflower shaped opaque areas beginning to form in the interior of the gel.

quickly. The rehydration characteristics of the large pore gels give an indication as to why this may occur.

2.2.7 Rehydration and Doping Gel Monoliths

The best way to rehydrate a gel is by immersing only the bottom of the gel in liquid. This allows the air in the pore network to escape through the top of the gel as demonstrated in Figure 2.10. Rehydration is usually rapid and without incident. If the gel is completely immersed in water, it will rehydrate more slowly since the air must diffuse out through the already filled pores. Experience has proven that the threshold pore size for successful rehydration of dried gels is in the vicinity of 70 -80Å. Gels with smaller pores can be stabilized at high temperatures to impart more strength and in some cases can be gain strength and often can be rehydrated without failure.

If, however, rehydration is interrupted for too long a period the gel will crack in the vicinity of the demarcation between the rehydrated and dry areas of the gel. The fracture occurs after a delay (up to several minutes depending on the speed of rehydration) attributable to the equilibration of the hydrated portion of the gel. This characteristic suggests that a maximum degree of stress is produced between the fully hydrated and empty or funicular areas within the gel. It also suggests a time related dependence. If the rehydration front is kept moving cracking is avoided. If it moves too slowly or stops, the gel cracks. Figure 2.11 is a series of photos illustrating what happens when the rehydration of a large pore gel is interrupted. Notice that although cracks extend out into the dry portion of the gel, the fracture surface itself occurs almost precisely along the rehydration boundary. Although there are significant differences between the drying scenario and the rehydration of gels, experience has shown that gels dried too slowly are more prone to failure just as gels dried too quickly. In fact, a rehydrated gel can be placed

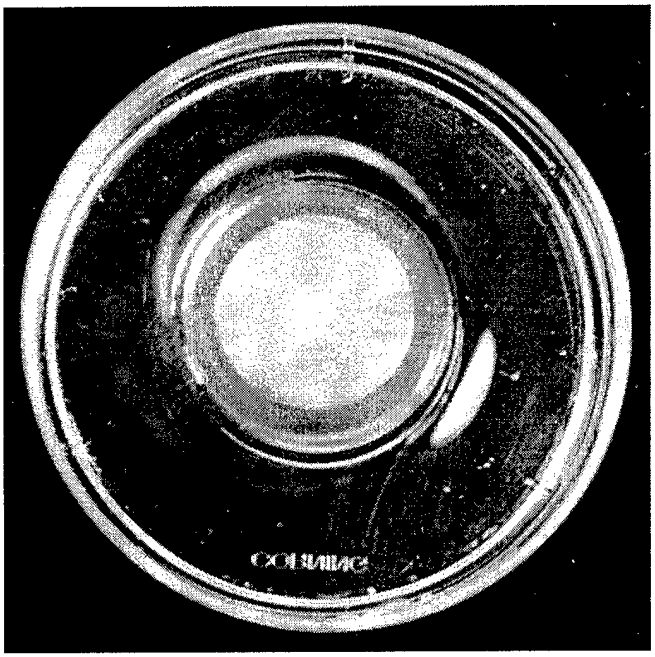

Figure 2.10. Large pore gel being rehydrated with water in a plastic dish. Notice the reduction in optical scattering as the liquid penetrates the gel.

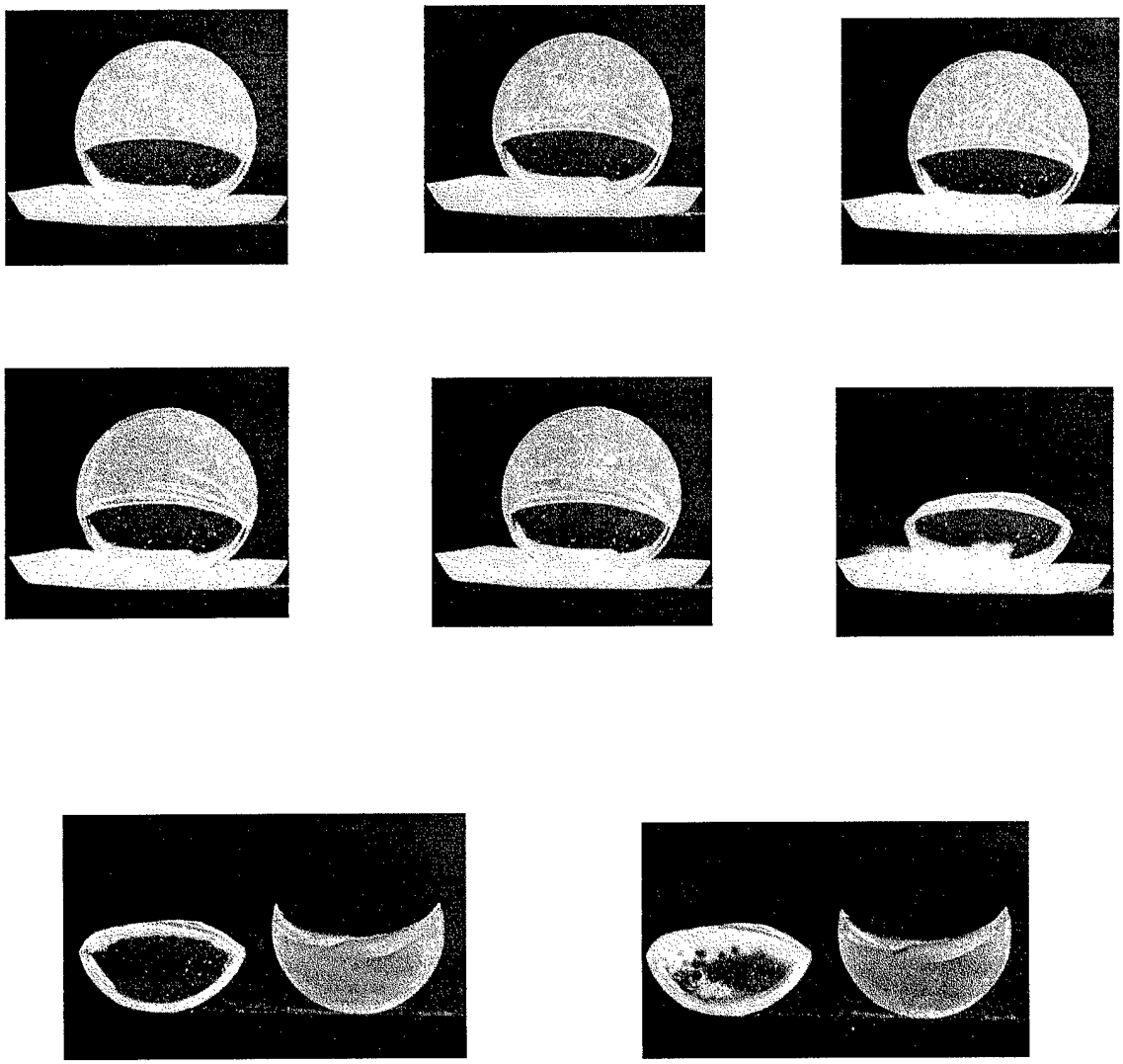

Figure 2.11. Series of photos illustrating what happens when rehydration of a large pore monolith is interrupted. Photos were taken approximately one minute apart after rehydration was interrupted by the removal of the water source. Although several cracks propagate into the dry portion of the gel, the fracture plane is precisely along the rehydration front. Note also the beginning of the opaque stage in the last two frames.

in a drying container and rapidly redried at 103°C without failure while the same gel if left to dry slowly at ambient temperature almost invariably will fail.

Once a gel has been rehydrated and removed from the solution it begins to dry. Opaque areas soon begin to appear and grow as water evaporates from the surface of the gel. The last two frames in Figure 2.11 show the opaque area begin to spread as the rehydrated portion of the gel begins to dry. Opaque areas have even been observed to begin in the center of a gel. Once the gel is entirely opaque it becomes insensitive to drying rate. As drying continues the gel (depending on pore size and scattering) once again becomes transparent or translucent.

2.2.8 Stabilization and Densification

The stabilization of large pore gels is very similar to their smaller pore cousins except that pore shrinkage and closure occurs at a higher temperature. There is little change in pore texture up to about 1000°C at which point densification begins. Due to their lower specific surface areas (typically 100 - 200 m^2/g vs 400 - 600 m^2/g for a 45Å gel) large pore gel monoliths are less hydrophilic and retain less water than higher surface area gels. A typical 200Å pore radius gel will pick up approximately 2% by weight in water vapor from the atmosphere as opposed to more than 6% for a 45Å gel. The greater permeability of large pore gels also allows water vapor to more readily escape during consolidation. In Addition, large pore matrices consolidate at higher temperatures than smaller pore gels. Consequently, the large pore monoliths can be brought to full density under ambient atmosphere without dehydroxylation treatments. Figure 2.12 shows the densification schedule for the system. Full density is normally achieved by heating the gels to 1150°C - 1200°C. Bloating can still be a problem with larger size pieces if the heating rate is too rapid but for the typical 2cm by 7mm disks it is infrequent. Large pieces are still difficult to dry intact hence data on their densification is limited.

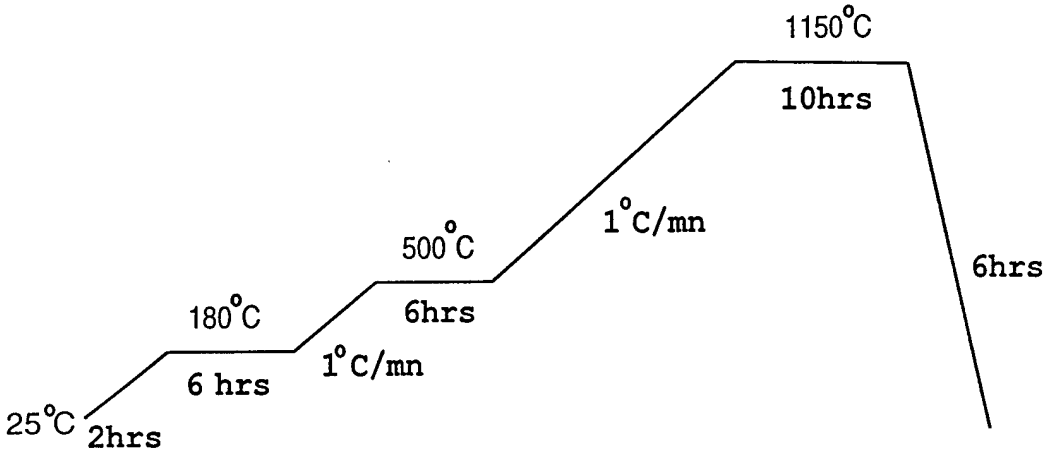

Figure 2.12. Standard densification schedule for large pore monoliths.

Dried monoliths are also machinable. They are relatively soft and can be cut dry with ordinary tools (such as a small band saw, or lathe) or shaped with a grinding wheel. They can then be densified as described above. Thus larger more intricately shaped pieces can be cut from a standard shaped cylinder (or even from larger fragments of a failed monolith).

2.3 Conclusion

The large pore gel system described here shows promise in several areas such as optical sensor substrates, catalyst supports and as preforms for dense high purity silica components. In the smaller size range (up to about 2.5cm by 1cm) they are easily manufactured with excellent yields (approx. 80%). Larger sizes are still difficult to produce. At a pore radius of 200Å, they retain enough transparency to be useful in optical sensing applications, can be easily rehydrated and redried without failure and can be reliably brought to full density. The relatively large pore size imparts good permeability and the large pore volume permits doping with a wide variety of materials. As shall be seen in the next chapter, the pore volume and surface area can also be modified in either direction.

CHAPTER 3
VARIATION OF PORE SIZE BY AGING AND DRYING

3.1 Introduction

The following experiments examine the modification of pore morphology by aging and drying treatments. Traditionally, aging has been used to strengthen the gel before drying and extended aging treatments have been used to increase the final pore size of the gel. Aging in high pH solutions (base aging) has been employed to increase the solubility of silica thus accelerating the Ostwald ripening process. Gel monoliths in the 100Å pore radius range have been routinely produced through this method.[9] It has been difficult to follow the evolution of the pore structure through the aging process since there is no easy way to freeze the pore morphology and remove the solvent without further modification of the pores. Conventional drying of gels dramatically alters the pore structure since it is essentially a form of high temperature aging up to the point at which the pores become pendular. The pore structure is also modified during the drying process through capillary pressures which create a compressive stress on the gel causing it to shrink. As the gel shrinks it continues to age in what is usually a high temperature acidic aqueous environment. The final pore structure is not determined until the pores begin to empty of solvent to reveal a dry gel. In the first experiment, supercritical drying is used to elucidate the change in pore structure at several steps throughout the aging process. The assumption is that by exchanging the pore solvent with methanol, the aging process is arrested due to the low solubility of silica in methanol. Supercritical drying is then used to remove the solvent leaving the pore structure relatively unchanged. The dried gel can then be analyzed by nitrogen adsorption to ascertain the surface area, pore size and distribution. By analyzing the gel at several points, a picture of the aging process can be constructed.

The second experiment examines the concept of aging silica gels in an acid environment in combination with a silica "donor" consisting of a high surface area silica gel. The concept explores the possibility of adding additional silica to the gel being aged to increase the strength and bulk density while decreasing the pore size. Thus the gel is modified to decrease in pore size. Though the pore size changes in the opposite direction, the objective is the same - to increase the strength and survival of gel monoliths.

The third experiment deals with the effect of gelation volume on the ultimate pore size of the gel. A fixed amount of sol is diluted to increase the volume of the gel while keeping the same solids content. At first one is inclined to think that increasing the gelation volume should increase the pore volume and hence the average pore radius. This turns out not to be the case.

3.2 The Evolution of Pore Structure During Aging and Drying

In this experiment the change in the pore structure of a standard large pore gel is determined at several steps in the aging and drying process through the use of supercritical CO_2 drying. The gel formulation was that of the "standard 200Å" formulation as recorded in Table 2.1 in the last chapter. Four samples were analyzed at four different stages of aging/drying.

3.2.1 Experimental

The starting solution was cooled to 15°C and the temperature rose to 31.5°C after the addition of the TMOS. After 8 minutes 10ml of sol was filtered into several 15ml PMP molds. The remainder of the sol was left to gel in the Teflon reaction container and aged and dried separately. After 2 hours and forty five minutes one gel was immersed in 250 milliliters of Fisher Optima grade 99.9% methanol with magnetic stirring in order to replace the pore liquor with methanol. The remaining gels were aged for 2 days at room

temperature followed by 24 hours at 70°C. The first gel was left in methanol with magnetic stirring for two days to allow adequate time for the solvent in the pores to equilibrate. The percentage of water in the equilibrated solvent was calculated to be no more than 1.5% by weight. The gel was then removed and supercritically dried in a SAMDRI 780 critical point CO_2 dryer designed primarily for drying biological samples for electron microscopy. After solvent exchange, the 20mm x 22mm cylindrical gel was placed in a specially constructed sample holder in the sample chamber of the critical point dryer. The sample chamber was cooled to 10°C and filled with liquid carbon dioxide. The sample chamber was kept between 0°C and 10°C and the CO_2 was purged and replaced every 10 minutes for 6 hours. The chamber was then heated to above 31° C and allowed to equilibrate. The pressure of the chamber was 1150 psi at this point. After 10 minutes the chamber was slowly purged of CO_2 over a period of 30 minutes. The resultant gel was then removed for analysis by nitrogen adsorption. Mercury and helium pycnometry was used to determine the bulk and structural densities of the aerogel.

The second sample was aged normally and dried up to the critical point. The critical point was identified by observing when the opaque stage had just begun to form on the surface of the gel. The sample was then removed from drying and immersed in methanol for solvent exchange. After the solvent was exchanged with methanol the gel was supercritically dried as described above. This gel remained intact and was analyzed similarly to the first.

Sample number three was derived by subjecting the gel to a normal aging and drying schedule. It also survived the drying procedure intact and was analyzed as described above.

The last sample was taken from the large monolith which was subjected to an extended drying schedule lasting 2 weeks. The large (600ml) monolith broke into several large pieces which were analyzed to determine pore structure. Figure 3.1 outlines the aging and drying schedules for each of the samples tested.

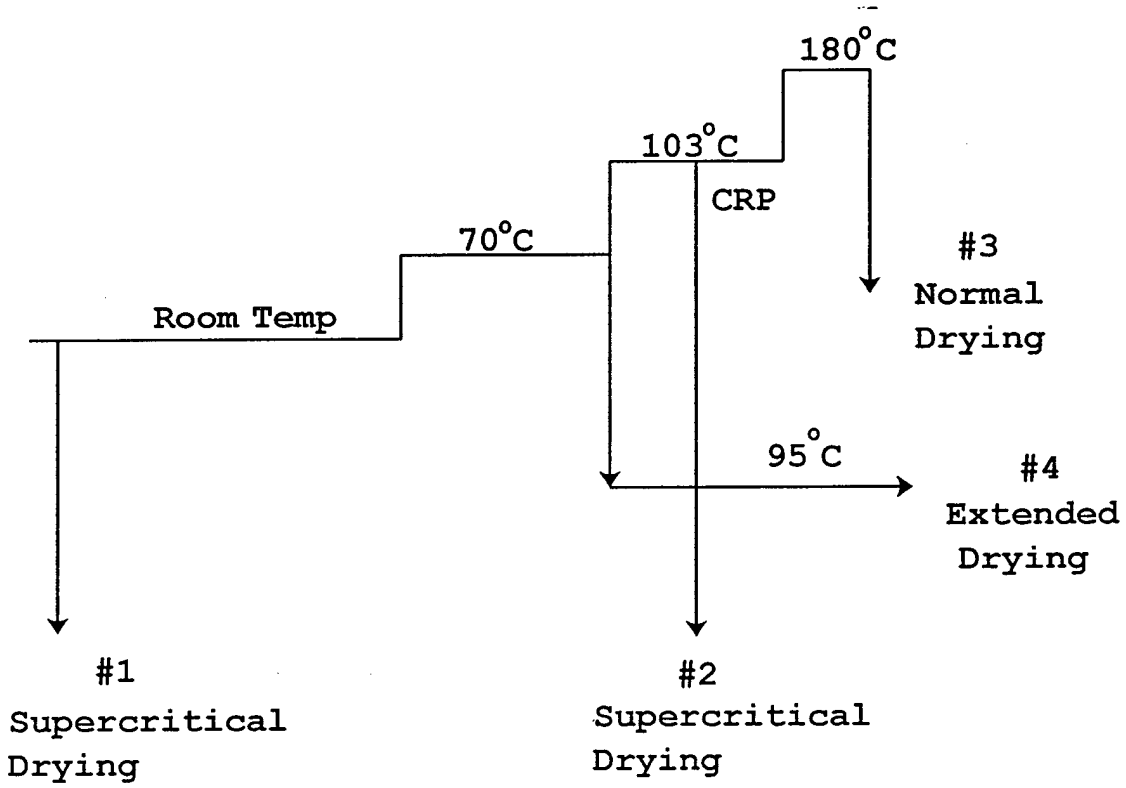

Figure 3.1. Schematic of aging and drying schedule for four gels taken from the same large pore formulation. Sample #1 was supercritically dried shortly after gelation. Sample #2 was supercritically dried after reaching the critical point (CRP) in the normal drying schedule. Sample #3 was analyzed after a standard drying schedule and sample #4 after extended drying due to the large bulk of the gel monolith.

3.2.2 Results and Discussion

Table 3.1 shows the variation in surface area, pore volume and average pore radius for each of the samples. Figures 3.2 through 3.5 show the isotherms and pore radius distributions of the four samples. As might be expected, the surface area decreases dramatically as the aging process continues. The most significant drop in surface area is between sample #1 and sample #2. This is understandable as it is during this time frame that the bulk of the aging process occurs. At the critical point (sample 2) all of the low temperature aging is completed and a significant amount of time has been spent at the drying temperature of 103 °C.

Consistent with acid catalysis of silicon alkoxides, the gel likely consists of small (3nm) colloidal particles immediately after gelation. Particles this small can be expected to have significantly greater solubility than bulk silica. This combined with high temperatures can be expected to accelerate the Ostwald ripening of the internal surface of the gel This is what occurs between sample 1 and sample 2. Samples 3 and 4 show a more moderate decrease in surface area only because the bulk of the aging process is completed.

The pore volume depends primarily on how the gel is dried. Sample one is characteristic of aerogels with a very large surface area and pore volume. Surprisingly, however, the average pore radius is only about 100Å. By the time the gel reaches the critical point in sample 2 most of the aging process is over and most of the shrinkage has been completed. The analysis of sample 2 closely resembles the pore structure of sample 3 even though they were dried by different means. The resemblance between the two gels substantiates the two assumptions made at the beginning of this experiment i.e. that aging slows or ceases upon replacing the solvent with methanol and that the supercritical drying process preserves the pore morphology of the gel at the time of solvent exchange. The gel supercritically dried at the critical point should differ from the one dried conventionally

Table 3.1. Pore characteristics of standard 200Å gels at various stages of aging/drying.

Sample	Surface Area (m^2/g)	Pore Volume (cc/g)	Average Pore Radius (Å)	Adsorption Peak Radius (Å)	Desorption Peak Radius (Å)
Sample #1 2:45 hrs Supercritical Drying	1020	5.095	99.93	(133.6) broad	52.5
Sample #2 Critical Point Supercritical Drying	186.1	1.97	211.4	231.6	135.9
Sample #3 Normal Aging and Drying	158.5	1.59	200.7	280.0	152.3
Sample #4 Extended Drying Schedule (2 weeks)	101.6	1.90	373.3	675.4	263.4

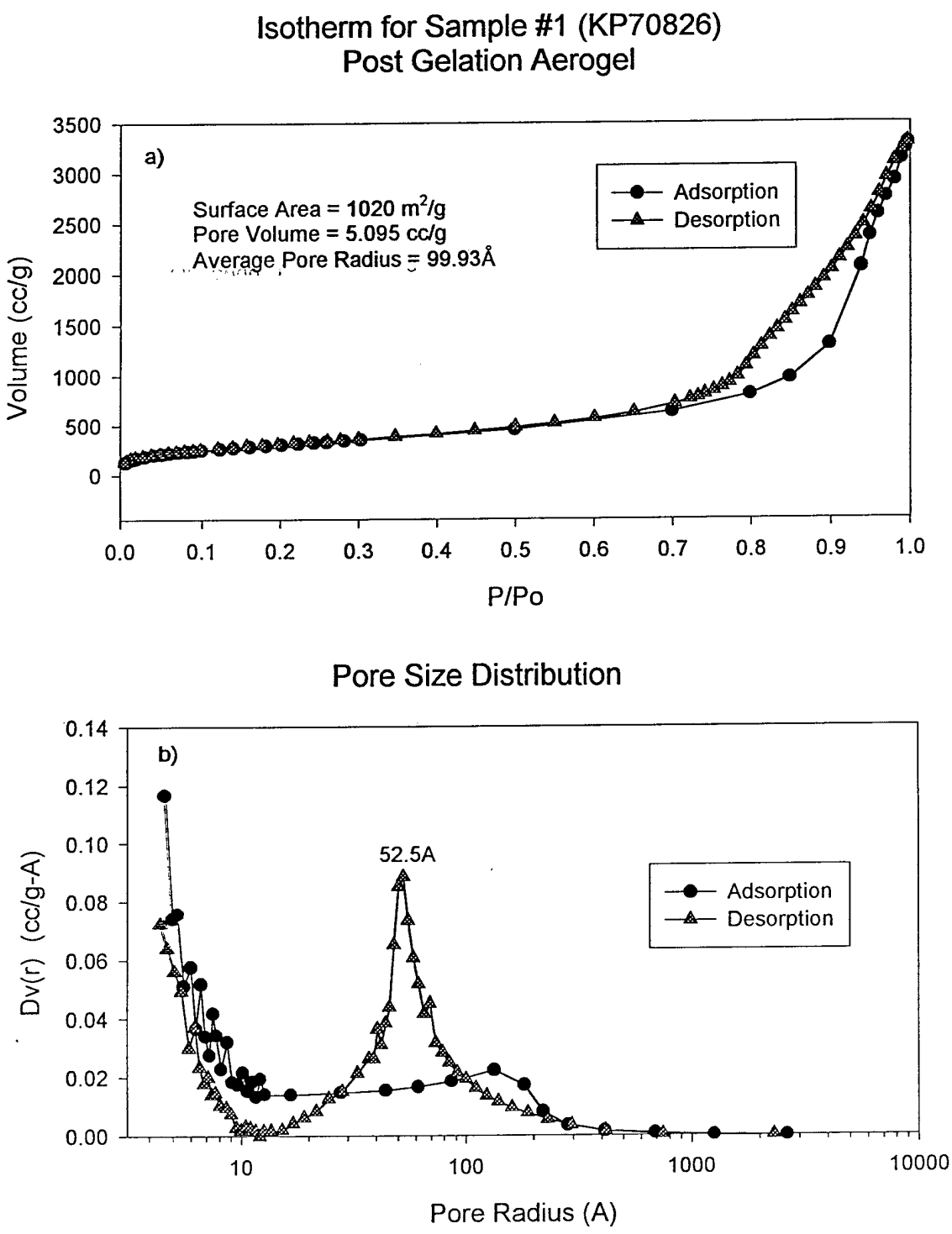

Figure 3.2. a) Isotherm for sample #1 (KP70826) solvent exchanged shortly after gelation and supercritically dried. b) Pore size distribution.

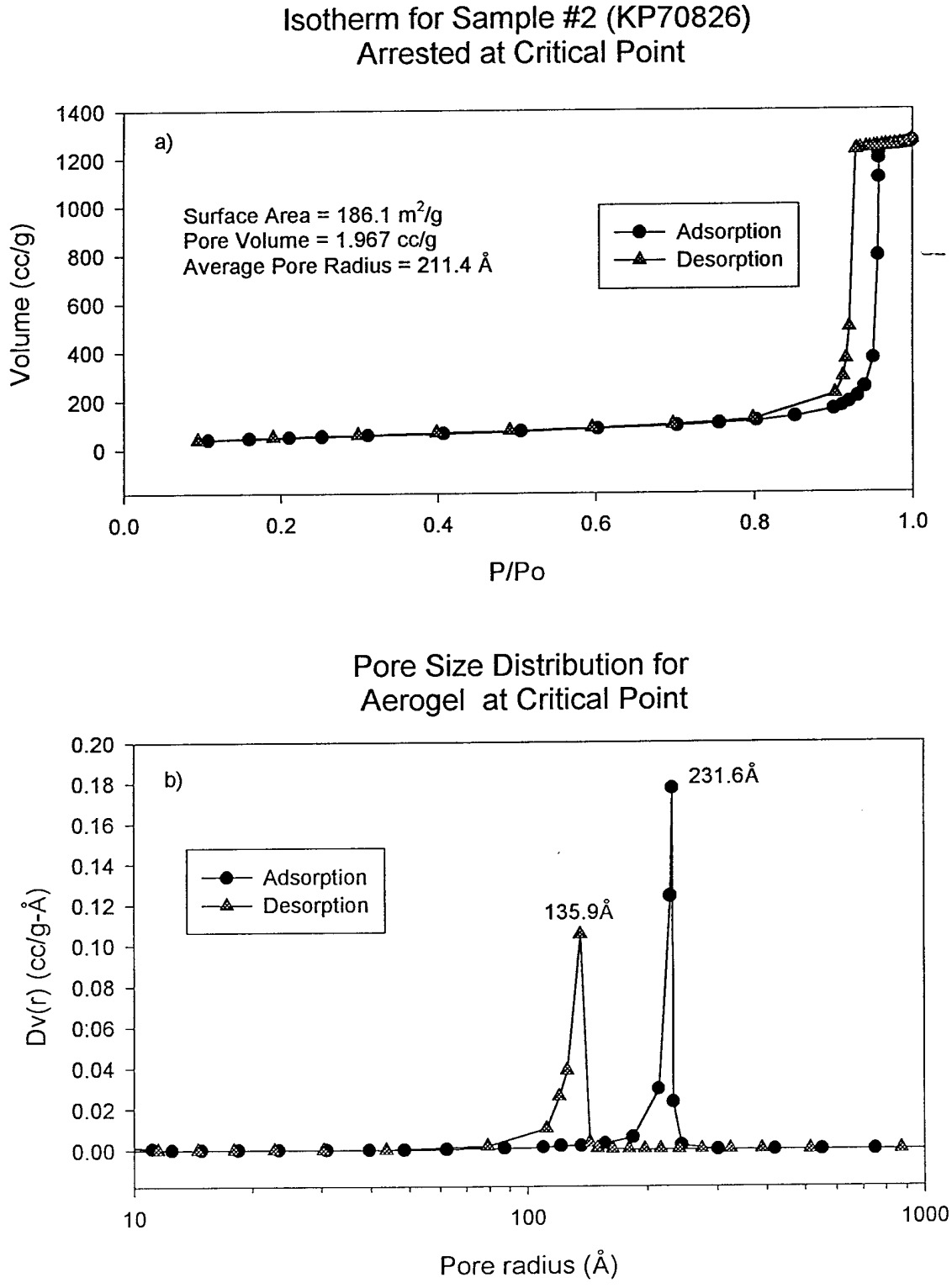

Figure 3.3. a) Isotherm for Sample#2, solvent exchanged after reaching the critical point and then supercritically dried. b) Pore size distribution.

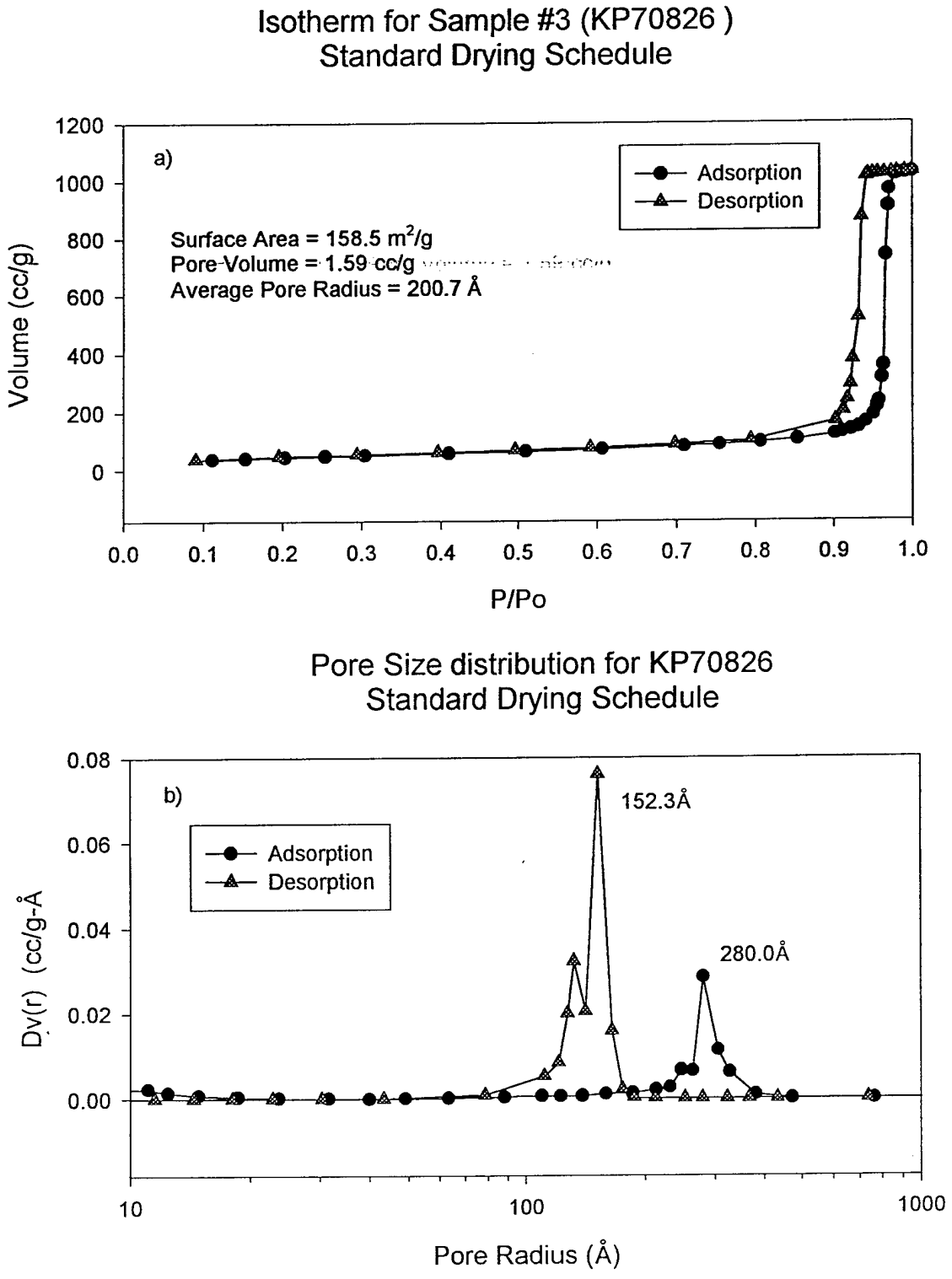

Figure 3.4. a) Isotherm for Sample #3, dried with standard drying schedule. b) Pore size distribution for Sample #3.

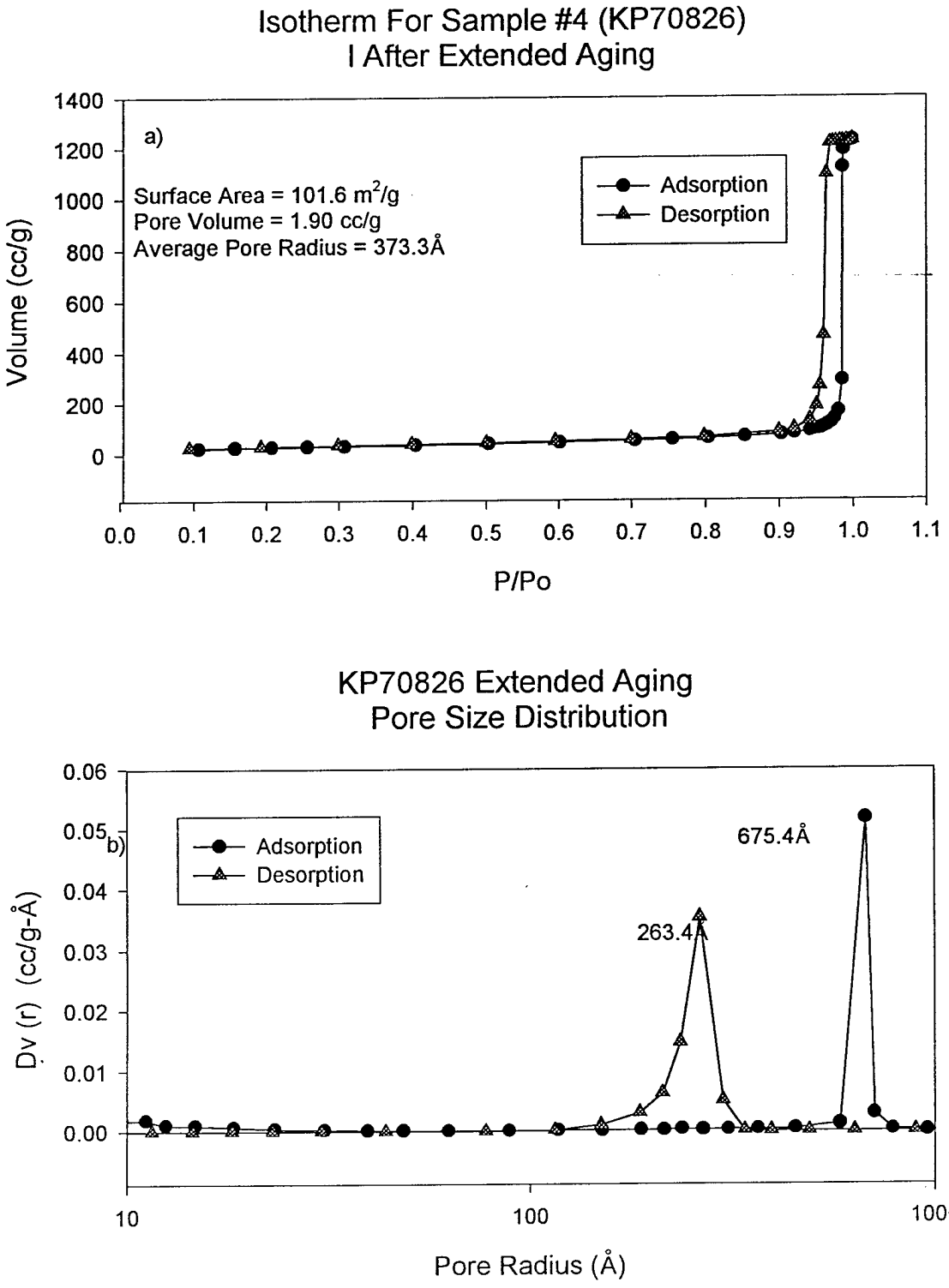

Figure 3.5. a) Isotherm for Sample #4 after 2 weeks extended aging and drying schedule. b) Pore size distributions for Sample #4.

only by the amount of aging which occurs during the emptying of the pores at 103°C. As can be seen, this is still significant but less so than the aging which has preceded it. The increase in pore volume with extended aging seen in sample 4 is attributable to an increased stiffness of the gel network as aging continues. With a stiffer network, the gel shrinks less on drying resulting in a larger pore volume.

Since the average pore radius is a ratio between the pore volume and the surface area assuming cylindrical pore shapes, it is not always representative of the actual size of the pore openings but can vary with the pore size distribution (pore volume increases as the square of the radius), pore shape (ink bottle shaped pores produce larger volumes with the same entry diameter) and the surface roughness (surface areas increase rapidly with surface roughness). Thus the average pore radius almost always falls above the peak desorption pore radius but it is the latter which most closely represents the pore entry size.

The isotherms for the four samples show the effect of the aging process on the adsorption of nitrogen and infer the changes that occur as aging proceeds. The isotherm for sample one (Figure 3.2) shows a broad adsorption/desorption range indicative of either a broad range of pore sizes or with a colloidal model considerable variability in the curvature of colloidal clusters. As the aging/drying time increases, there is a distinct steepening of the isotherms, displacement towards higher relative pressure and a more narrow adsorption-desorption gap.

The Pore size distributions paint a similar picture. As aging continues, the pore size gets larger and the distribution tends to become more narrow. Particularly notable is the change in the pore size distribution between sample 1 and sample 2 where the bulk of the aging process has already taken place. Figure 3.6 shows the pore size distributions for all four samples on the same axis for comparison.

3.2.3 Conclusions

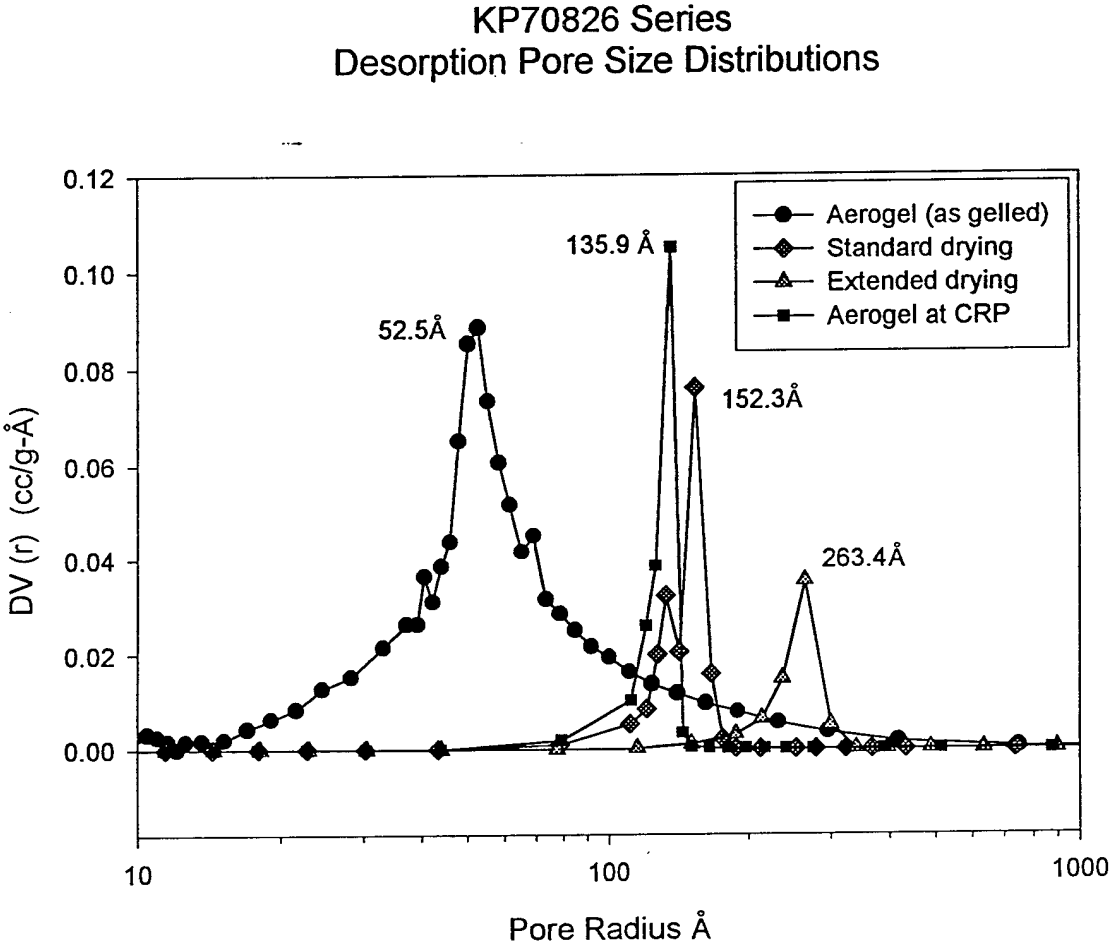

Figure 3.6. Desorption pore size distributions for HF catalyzed gel dried by four different methods. Supercritical CO_2 drying was applied to two gels, one shortly after gelation and the other at the critical point. the third gel was dried with the standard drying schedule and the last was part of a large monolith dried over a period of two weeks.

This experiment demonstrates the usefulness of critical point drying in determining the pore morphology of silica gels as they change in response to the aging and drying process. The pore structure of gels in the early stages of aging can be preserved by methanol replacement, and then analyzed by nitrogen adsorption after supercritical drying. Results demonstrate a classical Ostwald aging process whereby the surface area decreases with time, temperature and the increased water concentration. The pore volume is dependent primarily on the capillary induced shrinkage of the gel monolith which in turn is dependent on the size of the pores, the stiffness of the network and the drying method.

3.3 Pore Size Modification by Sacrificial Aging

In the course of several attempts to reinforce gel monoliths, it was discovered that aging a gel in the presence of a sacrificial silica donor resulted in smaller pore sizes and denser gel monoliths. Figure 3.7 is a diagram of the process as applied in a preliminary experiment. The large pore gel is modified toward higher surface area, smaller pore volume and a smaller pore radius while the seed gel shows decreased surface area, larger pore volume and a larger average pore radius (as would be expected through Ostwald ripening). Figure 3.8 shows the pore size distribution of both gels before and after the aging treatment. Note that although the pore size distribution of the seed gel grows larger, that of the large pore gel gets dramatically smaller.

This represents a possible avenue for increasing the surface area of dried xerogels by incorporating an additional source of silica in the aging process. There are at least two possible reasons for the effect. It's possible that silica is being deposited from the seed gel into the gel being aged in such a way as to increase the surface area (and possibly increasing the thickness of the pore walls). Another possibility is that the presence of the seed silica serves only to retard the aging of the gel as it is dried. As evidenced by the

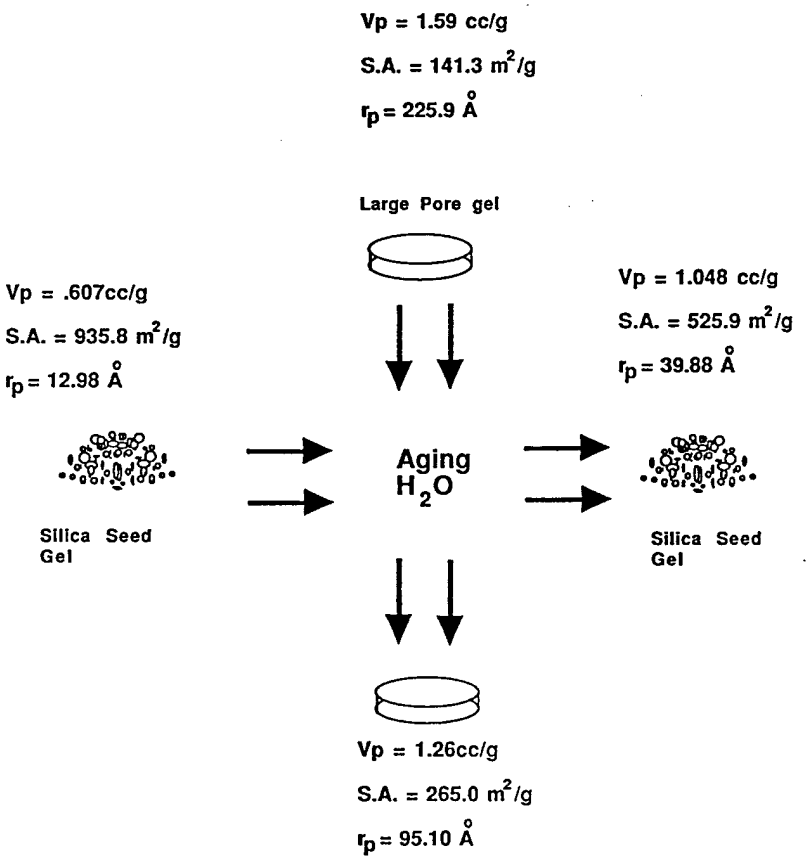

Figure 3.7. Schematic showing the pore modification of a large pore gel aged and dried in the presence of a high surface area "seed" gel.

experiment in section 3.2, the wet gels start out with a very large surface area (1020 m^2/g in the case of sample 1) which dramatically decreases during the aging and drying process. In either case, the result is a dried gel with a greater surface area and smaller pore volume. The following experiment examines the aging of a 200Å formulation using a high surface area silica gel donor.

3.3.1 Experimental.

In this experiment a standard 200Å batch of gels was prepared according to the same procedures in section 3.2.1. They were cast in 60ml PMP containers with Polypropylene screw on tops, aged at room temperature for 2 days and then aged at 70° C for 24 hours per standard procedure. Each gel consisted of 15ml of sol which has a nominal silica content of 1.5 grams. The seed gel was a commercial silica gel powder produced by Aldrich. Nitrogen adsorption was performed to characterize the seed gel. It had a surface area of 400m^2/g, a pore volume of .7618 cc/g and an average pore radius of 38.05Å. Twelve aged gels were separated into two groups of six each. To each gel of the first group was added 1.6 grams of seed gel and 40 ml of deionized water. The second group served as the control group and was aged under the identical conditions without the seed silica. Since the aged gels still contained pore liquor from the gelation process the resulting solutions were acidic with a pH of 1.85±.06.

All of the gels were tightly capped to prevent evaporation and placed in an oven at a constant temperature of 90°C to age. They were aged for varying amounts of time according to the schedule in table 3.2. After aging for the appropriate amount of time the gels were cooled, washed in deionized water and placed in a Teflon drying container. The standard drying schedule depicted in Figure 2.2 was used to dry the gels. The gels were then analyzed by nitogen adsorption to determine the pore characteristics after different aging times both with and without the presence of the silica seed.

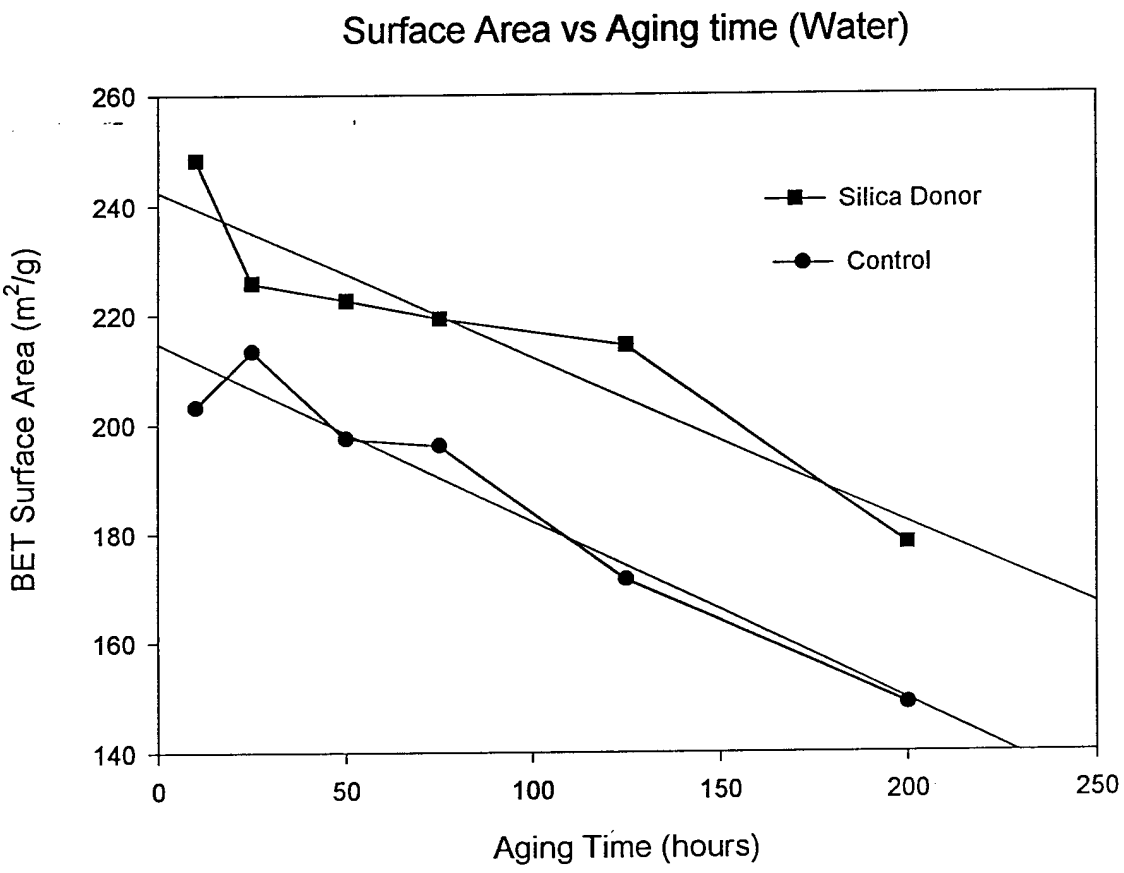

Figure 3.8. The change in BET surface area as a function of time for a standard 200Å formula gel aged with 1.6 grams of a high surface area silica gel. The control is from the same batch but aged without the seed gel.

3.4.2 Results andDiscussion.

Figure 3.8 shows the change in surface area of the gels with respect to aging time. The surface area the gels aged with the high S.A. silica seed is significantly larger than that of the control gels throughout the aging process. Both the silica seeded gels and the control gels show a decrease of surface area with aging time as one might expect from the Ostwald ripening process. The general slope of the curves for both sets of gels is similar. The plots of pore volume and average pore radius shown in Figure 3.9 are less definitive. The pore volume after drying is not directly related to the change in surface area but is determined to a large extent by the pore size (capillary forces), stiffness of the gel at the critical point, and the conditions of drying. There are several interesting aspects of the pore volume curves. The gels aged with the silica donor have smaller pore volumes in all cases. This can be indicative of seed silica being deposited in the gels and thus physically reducing the pore volume or simply the result of increased shrinkage during drying. However, contrary to this trend one would expect the deposition of additional silica in the gel to fortify the pore walls and fill in high radius necks between particles thus increasing the stiffness of the gel. This would tend to increase the pore volume during drying. The other interesting aspect of the pore volume plot is the way in which the pore volume of both the seeded gels and the control gels mirror one another throughout the aging process. Random variance in aging or drying conditions would not tend to produce curves of identical shapes as depicted. The maximum pore volume at 50 hours is the most intriguing and may indicate a point of particular significance. The average pore radius shows a general trend upward with aging time. Since the average pore radius is determined by the ratio of pore volume to surface area, it looks very similar to the pore volume plot.

3.3.3 Conclusions

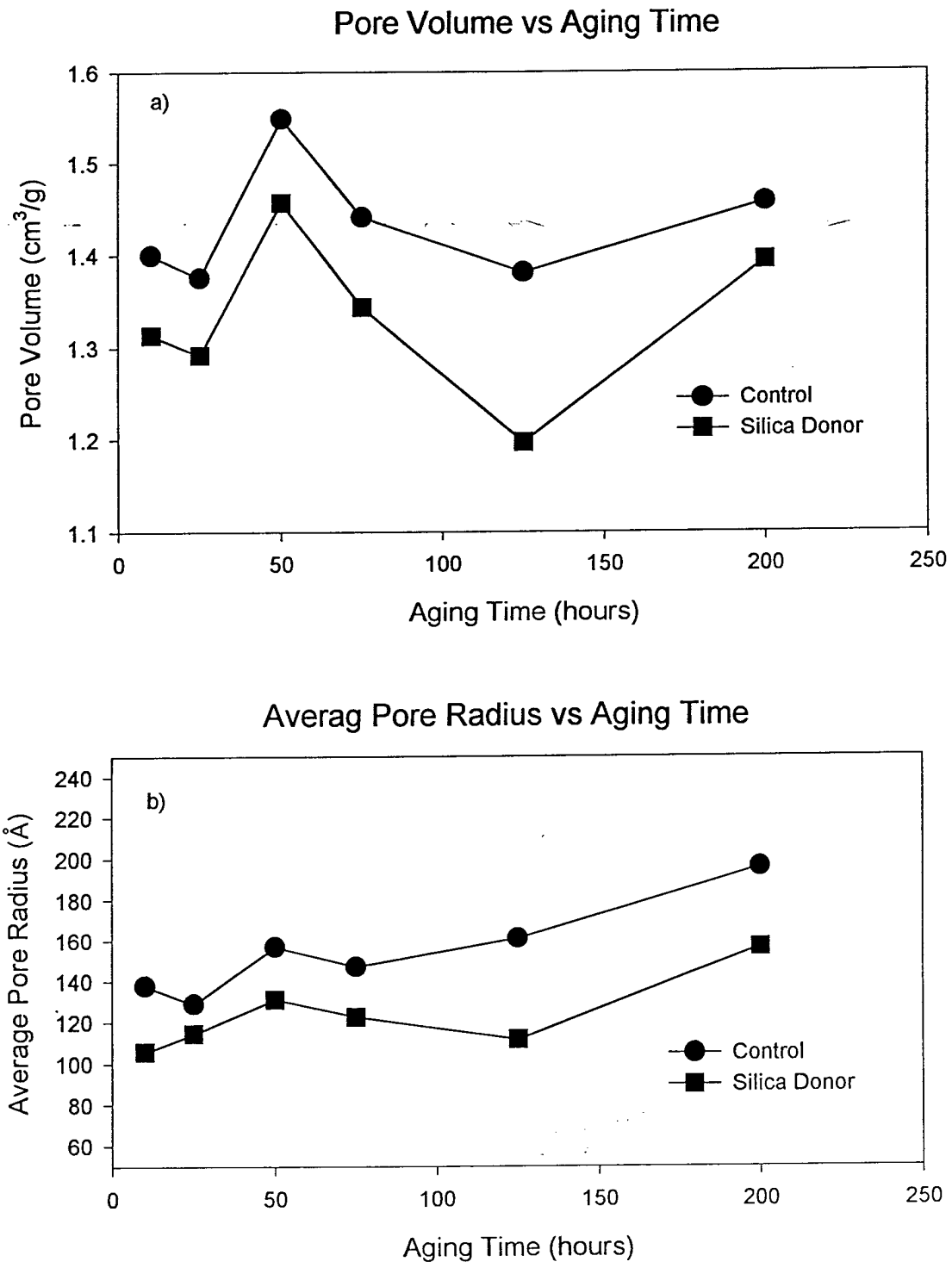

Figure 3.9. a) Pore volume versus aging time for gels aged with and without added donor silica. b) Average pore radius for the same gels as a function of aging time.

Because of the large number of variables in the aging and drying process, it is difficult to draw firm conclusions regarding the addition of seed silica to the aging solution. It is clear that doing so results in a higher surface area gel with a lower pore volume and consequent smaller pore radius. It is not immediately clear that this is due to the deposition of silica from the donor gel. This experiment was performed on very fragile wet gels which could not be accurately weighed before and after aging. Although the transfer of silica from the seed gel to the aging gels could account for the changes observed, they might also be due to a simple retardation of the aging process due to a higher concentration of soluble silica.

3.4 Effect of gelation volume on pore texture.

In this experiment the gelation volume of a silica gel monolith is altered by adding methanol in different amounts to a fixed quantity of sol, allowing the resulting solution to gel, and then subjecting the gel to a standard aging and drying schedule. The gels are then analyzed to determine the effect of gelation volume on ultimate pore texture.

3.4.1 Experimental

In this experiment the standard 200Å pore radius formula was again used. The starting solution was cooled to 16°C and the temperature rose to 35°C after the addition of the TMOS. 5 minutes after mixing, 10 milliliters of sol was filtered into 60ml PMP molds. 99.9% methanol (Fisher Scientific) was added to each jar in increments of 1 milliliter and the molds were tightly capped and then set aside to gel. Gelation volumes ranged from 10ml to 20ml. All of the gels contained the same amount of silica solids. As expected the dilution of the sol slowed down the gel time in direct proportion to the added methanol as depicted in figure 3.10. The solutions were all gelled within 2 hours and were

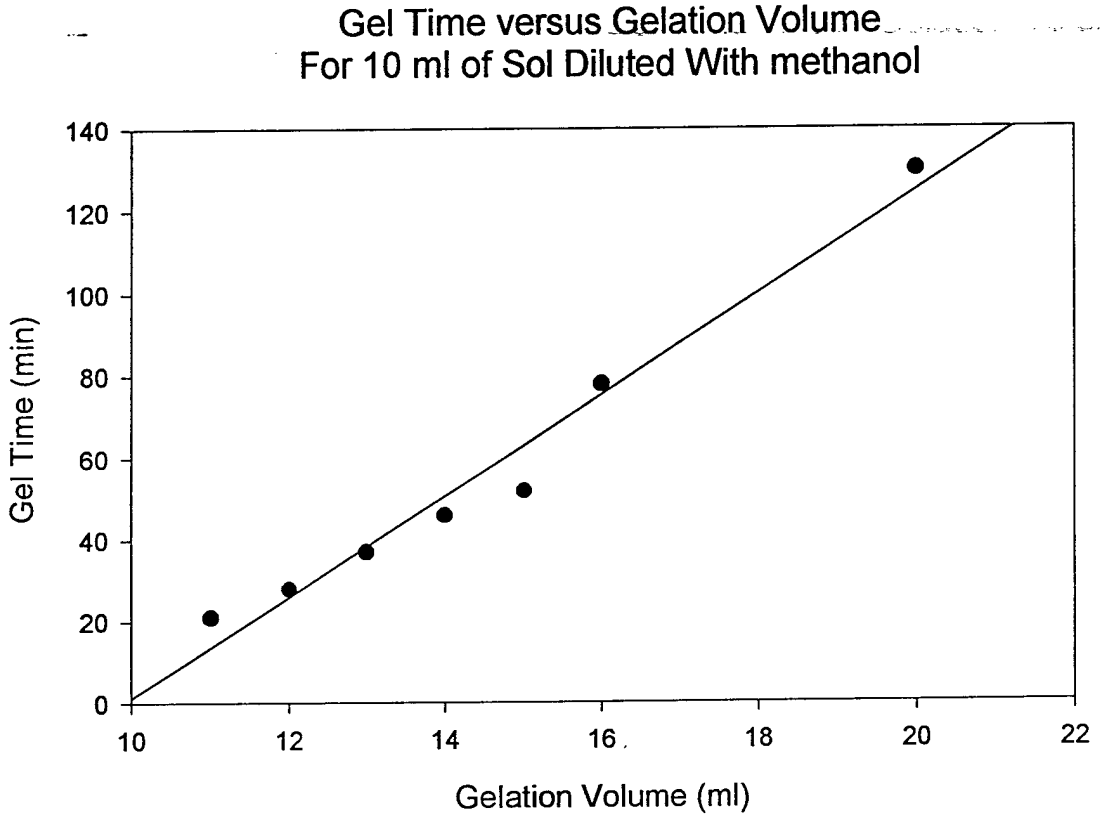

Figure 3.10. Gelation time versus gelation volume. Approximately 5 minutes after mixing, 10 milliliters of sol was diluted with methanol to the indicated volume and allowed to gel.

subsequently aged for 2 days at room temperature. After room temperature aging, the gels were placed in an oven and aged for another 24 hours at 70°C. Due to the mechanical weakness and high methanol content of the gels they were left in the PMP containers and heated at 70° until dry. (One gel, the 20ml gelation volume, was dried under standard conditions (see figure 2.2) to assess the effect of the unconventional drying schedule.) They were they transferred to Teflon containers and heated to 180°C to drive off physically adsorbed water and residual nitric acid before BET analysis.

3.4.2 Results and Discussion.

Figure 3.11 shows the results of the nitrogen adsorption pore texture analysis of the gels with the surface areas and pore volumes plotted as a function of gelation volume. It is clear that within the limits of nitrogen analysis (approximately ±5%), there is no significant change in either of these values as the gelation volume is varied through the addition of methanol. The gelation volume varies by factors of up to twice the initial volume, however by the time the gels are dried, they all achieve roughly the same surface area and volume. During the drying process, the gels shrink as the pore liquor evaporates until such time as the stiffness of the silica network is sufficient to resist the capillary pressures. As discussed in Chapter 2, when the gels reach the critical point the liquid meniscus begins to penetrate the pores. This is the beginning of the opaque stage. For these gels, such a large decrease in volume during drying necessitates a dramatic rearrangement of the aggregates - essentially a collapse of the structure into the smaller volume. The pore radius is plotted versus the gelation volume in Figure 3.12. All of the gels (except the 20ml which was dried at higher temperature) have average pore radii within 15Å of the mean at 198.3Å.

The relative uniformity of surface area is also significant. If one views the gel as a colloidal body of uniform sized colloidal spheres or aggregates, the surface area could be

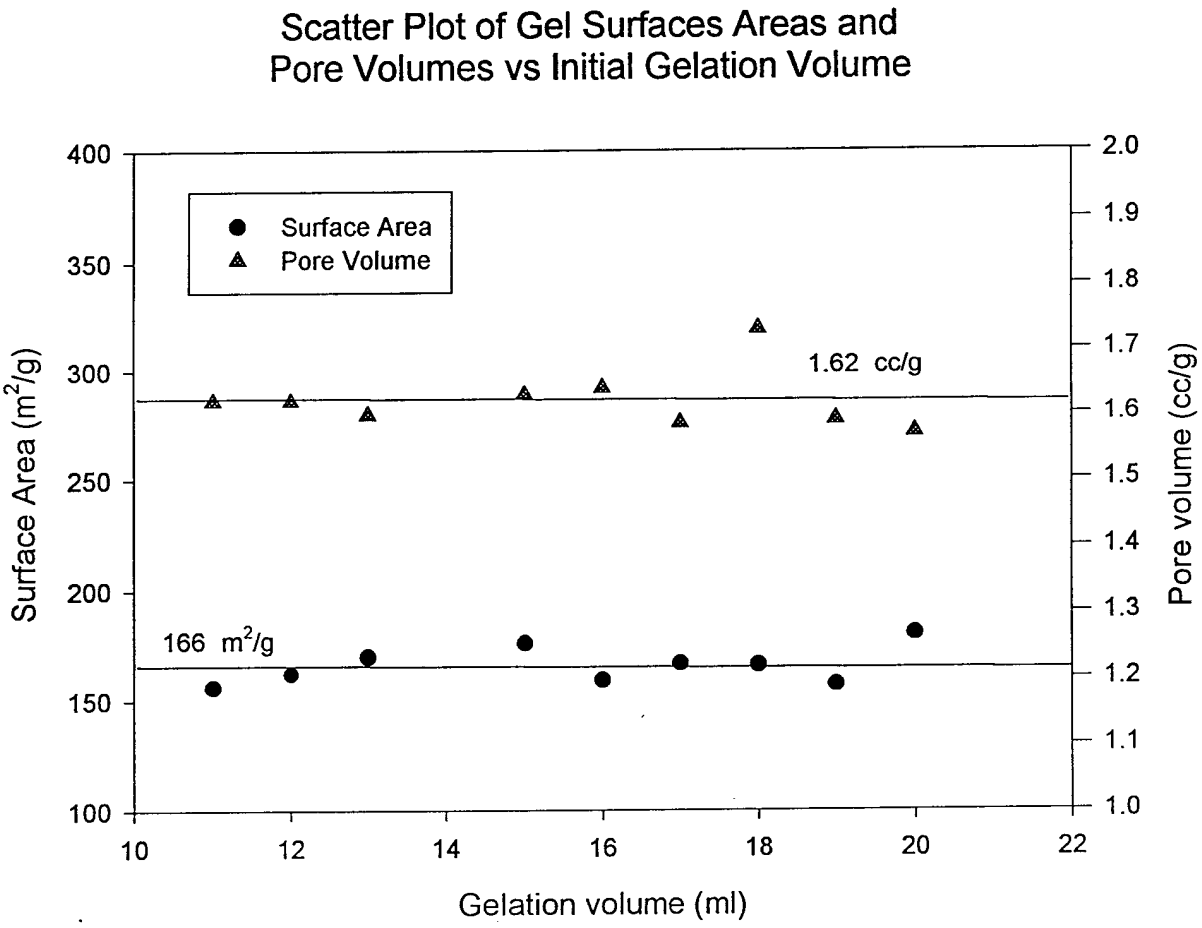

Figure 3.11. Surface area and pore volume of silica gels composed of 10 ml of a standard sol diluted with methanol to the indicated volume and allowed to gel. Gels were all aged according to the standard schedule in Figure 2.2 but dried at a reduced temperature of 70°C.

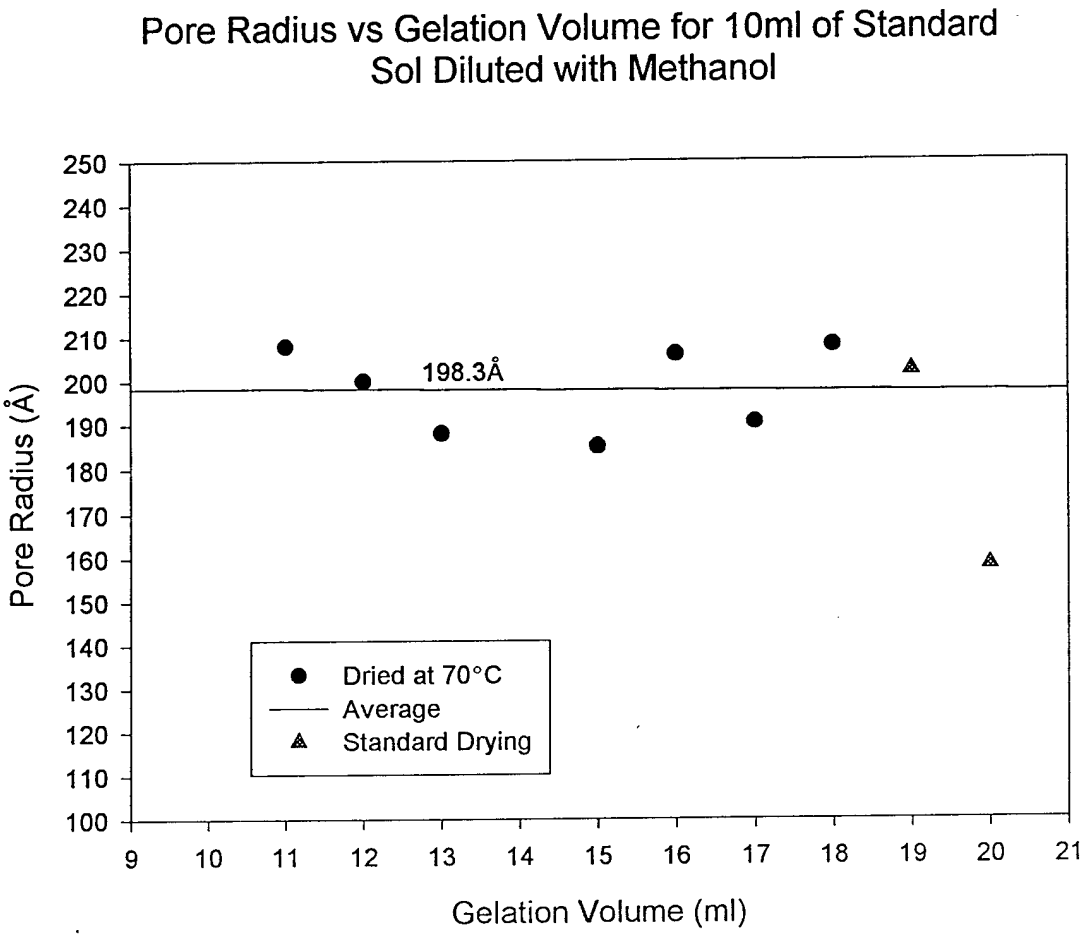

Figure 3.12. Pore radius versus gelation volume for gels diluted with methanol and allowed to gel at different volumes. Solids loading is the same for all gels.

expected to change due to Ostwald ripening at a rate dependent on the size of the colloids and the solubility of the silica in solution. This rate would be similar under similar conditions of aging and drying regardless of the initial arrangement of the colloids.

3.4.3 Conclusions

These results suggest the following scenario. The gels are made up of colloidal particles which during the aging process form agglomerates and are subjected to Ostwaldripening. As stress is applied by capillary forces, these aged agglomerates collapse into a randomly packed structure which is further strengthened (fused) by additional aging as the gel dries at elevated temperatures. When the gel achieves sufficient strength the collapse of the network ceases the pores empty of liquid and the final pore structure is preserved in the dry gel. The interesting aspect of this scenario is that such a collapse requires the fracture of the whatever necks may have already formed between agglomerates. Thus the shrinkage of the gel can be viewed as a process by which the necks between agglomerates progressively collapse and are reformed (by Ostwald ripening) until the network strength reaches a critical value at which point (the critical point) the gel is strong enough to resist the capillary pressures of the penetrating liquid. If this is indeed the case, it is no wonder why silica gels are so difficult to dry intact! This scenario also suggests a strategy for strengthening gels. If the gel is brought to the critical point and allowed to age predominantly at this minimum volume, it may be possible to produce gels more resistant to fracture.

References

1. L. L. Hench and J. K. West, *Chem. Rev.*, 90, (1990), p33.

2. H. P. Hood and M. E. Nordberg, U.S. Patent, 2,106,744, Feb 1938.

3. H. P. Hood and M. E. Nordberg, U.S. Patent, 2,286,275 , Feb 1942.

4. T. H. Elmer, in Engineered Materials Handbook®, Volume 4: Ceramics and Glasses, ASM International, Materials Park, Ohio, (1992), p427.

5. M. Ebelmen, *Ann. Chimie Phys.*, 16(1846), p129.

6. R.K. Iler, The Chemistry of Silica, Wiley, New York, (1979).

7. C. J. Brinker and G. W. Scherer, Sol-Gel Science, The Physics and Chemistry of Sol-Gel Processing, Academic Press, Inc., New York, (1990).

8. H. E. Bergna, in The Colloid Chemistry of Silica, H.E. Bergna, Ed., American Chemical Society, Washington, DC (1994), pp.147-159.

9. J. Fricke, Aerogels, Springer Proceedings in Physics, Vol 6, Springer Verlag, Heidleberg, FRG, (1986).

10. W.Q. Cao, and A. J. Hunt, *App. Phys. Lett.*, 64, (1994), p2376.

12. S.J. Gregg and K. S. W. Singh, Adsorption, Surface Area and Porosity, 2nd Ed, Academic Press Inc., London, (1982).

13. Quantachrome Corporation, Operations Manual for the Autosorb 6 Nitrogen Sorption System, (1985).

14. D. N. Winslow, in Surface and Colloid Science, Vol 13, E. Matijevic and R. J. Good Eds., Plenum Press, New York, (1984), p259.

15. S. Wallace, Porous Silica Monoliths, Structural Evolution and Interactions with Water, Dissertation, University of Florida, (1991).

16. L.L. Hench and J. W. West, Principles of Electronic Ceramics, Academic Press Inc., New York, (1990).